NEW HEXADENTATE ANCILLARY LIGANDS AND THEIR METAL ORGANIC COORDINATION NETWORKS

Gaurav Verma

A dissertation submitted for the partial fulfillment of B.S.-M.S. Dual Degree in Science

Indian Institute of Science Education and Research Mohali

April 2014

Certificate of Examination

This is to certify that the dissertation titled "New Hexadentate Ancillary Ligands and Their Metal Organic Coordination Networks" submitted by Mr. Gaurav Verma (Reg. No. MS09053) for the partial fulfillment of BS-MS dual degree programme of the Institute has been examined by the thesis committee members duly appointed by the Institute. The committee finds the work done by the candidate satisfactory and recommends that the thesis be accepted.

Prof. Ramesh Kapoor	Dr. Ramesh Ramachandran	Dr. Sanjay Mandal
(Member)	(Member)	(Convener & Supervisor)

Dated: April 25, 2014

Declaration

The work presented in this dissertation has been carried out by me under the guidance of Dr. Sanjay Mandal at the Indian Institute of Science Education and Research Mohali. This work has not been submitted in part or in full for a degree, a diploma, or a fellowship to any other university or institute. Whenever contributions of others are involved, every effort is made to indicate this clearly, with due acknowledgement of collaborative research and discussions. This thesis is a bonafide record of original work done by me and all sources listed within have been detailed in the bibliography.

Gaurav Verma

Dated: April 25, 2014

In my capacity as the supervisor of the candidate's project work, I certify that the above statements by the candidate are true to the best of my knowledge.

Dr. Sanjay Mandal

Dated: April 25, 2014

Acknowledgements

I would like to thank my supervisor Dr. Sanjay Mandal for providing me this opportunity to work with him and for the knowledge imparted to me. Special thanks go to Dr. Sadhika Khullar for her valuable comments and guidance throughout the project. I would also like to thank Sandeep for all the help and inputs provided during the project work. I thank my labmates Navnita, Biswajit, Vijay, Karan, Gouri, Datta and Prasenjit for their support and help.

I also thank my friends Harsh, Mayank Chugh, Ashutosh Tripathi, Sudeep, Nirdosh, Nayyar bhaiya, Ashutosh Tiwari, Akshey, Shiven, Ashwani bhaiya, Pallavi didi and many others who provided moral support and help to me through all these years. I take this opportunity to thank Mangat bhaiya, Bahadur bhaiya and Satwinder bhaiya.

I would like to thank IISER Mohali for providing with all the facilities. I am grateful to MHRD for the INSPIRE fellowship for the duration of my study here.

Finally, I would like to thank my parents, brother, entire family and above all God.

List of Figures

List of Schemes

List of Tables

Contents

Abstract

Two new hexadentate ligands, N, N', N'', N'''-tetrakis-(4-pyridylmethyl)-1,4-diaminobutane (4-pytpbn) and N,N''-bis-(2-pyridylmethyl)-N',N'''-bis-(4-pyridylmethyl)-1,4-diaminobutane (2,4-pytpbn) have been synthesized and structurally characterized. Complexes of 4-pytpbn of the general formula [M(4-pytpbn)X_2], where M^{2+} = Co^{2+} (**1**, **2**, **5**), Cd^{2+} (**3**), Cu^{2+} (**4**); X^- = NO_3^-, Cl^-, ClO_4^-, and [M_2A_2(4-pytpbn)], where M^{2+} = Zn^{2+} (**6**), Cd^{2+} (**7**) and Ni^{2+} (**8**, **9**), A^{2-} = adc^{2-}, fum^{2-}, $succ^{2-}$, have been synthesized. All these complexes have been characterized by elemental analysis, FTIR spectroscopy, thermogravimetric analysis and powder X-ray diffractometry. Single crystal X-ray analysis of the ligands and preliminary results of **1** and **2** that establish the presence of expected pores in these are also reported.

Chapter I

Introduction

Over the past few decades, a new class of novel functional materials has emerged.[1] These are usually crystalline compounds built from multi-dentate organic ligands/linkers and metal ions or clusters. These components are held together by coordinate bonds and/or weak interactions such as hydrogen bonding, π-π stacking, etc., to form extended 1D, 2D or 3D infinite network structures and are of particular interest due to the wide structural adaptability and tenability of the structures obtained. In principle, a wide range of structural, optical, electrical, magnetic, and catalytic properties can be incorporated into the frameworks by rational design.

Metal organic coordination complexes date back to Werner's type complexes containing octahedral transition metal complexes and nitrogen-metal coordination bonds.[2] The term coordination polymer was first used in 1916.[3] Prior to the 1980s, a variety of polymeric coordination compounds as Hofmann type complexes and Prussian blue compounds were discovered and these examples inspired development of strategies aimed at finding new class of materials.[4] In 1989, Hoskins and Robson proposed the design of open framework based on node and spacer approach.[5] Subsequently, in 1990s research on metal-organic hybrid frameworks increased and reports by R. Robson[5,6], S. Kitagawa[7], M. Fujita[8], M.J. Zaworotko[9], O.M. Yaghi[10] and Moore[11] established possibilities for new polymeric material structures and properties. The term metal organic frameworks (MOFs) was popularized around 1995 by O.M. Yaghi et al. in connection with the three dimensional porous coordination networks.[12] In 1999, S. Kitagawa reported gas adsorption properties of these porous coordination networks.[13]

Since then, research in this field has seen tremendous growth and an enormous amount of these materials have been synthesized and explored for their potential applications as gas storage materials, drug delivery agents, sensors, probes, catalysts and explosives, etc.[14]

Diversity of the materials synthesized and reported from an infinite number of combinations has led to a variety of terminological use for these materials, causing confusions and unnecessary misunderstandings.[15] To resolve the ambiguity, International Union of Pure and Applied Chemistry (IUPAC) initiated a project in 2009 to give a nomenclature and classification for these

materials.[16] The IUPAC task group, Coordination Polymers and Metal Organic Frameworks: Terminology and Nomenclature Guidelines, has since then documented, analyzed, and evaluated existing practices and recommended the following definitions:[15]

Coordination Polymer: A coordination compound with repeating coordination entities extending in 1, 2, or 3 dimensions.

Coordination Network: A coordination compound extending, through repeating coordination entities, in 1 dimension, but with cross-links between two or more individual chains, loops, or spiro-links, or a coordination compound extending through repeating coordination entities in 2 or 3 dimensions.

Metal Organic Frameworks (MOFs): A metal–organic framework is a coordination network with organic ligands containing potential voids.

Unfortunately, a lot of confusion prevails and often these terms are used interchangeably. Recently, a new classification for these materials, metal organic coordination networks (MOCNs) is in use.[17,18] MOCNs include the coordination polymers, supramolecular assemblies and metal organic frameworks (MOFs). Coordination polymers and metal organic frameworks are defined as above, supramolecular assemblies are networks formed via non-covalent interactions, such as hydrogen bonding, π-π interactions, etc., to give highly organized structures. A series of three dimensional MOCNs[17] and self assembled two dimensional MOCNs on metal surfaces have been reported.[18]

Design and Synthesis of MOCNs

MOCNs are constructed from three key components: inorganic connectors, ancillary ligands and organic linkers. Inorganic connectors are the metal ions (primarily transition metals and lanthanides) having multiple coordination sites such as Zn(II), Cd(II), Cu(II); ancillary ligands, such as 2,2-bipyridine, satisfy coordinative unsaturation of the metal ion and provide tenability in the structure of the network; and organic linkers, like terephthalate, afford a variety of linking sites with tuned binding strength and directionality. Sometimes counter anions can be present to balance the charge on the metal ion. These can be both outside the sphere like ClO_4^-, or chelating

to the metal ion like NO_3^-. Guest molecules which are generally solvent molecules, such as H_2O, CH_3CN, can sometimes be trapped inside the framework.

Different metal ions prefer different coordination numbers and geometries, such as linear, T- or Y-shaped, tetrahedral, square planar, square pyramidal, trigonal bipyramidal, octahedral, trigonal prismatic, and pentagonal bipyramidal (Figure 1). For example, Cu(II) ions having d^9 electronic configuration prefer square planar and tetrahedral geometries, but depending on the choice of ligand(s) and solvent(s), can be found with other coordination geometries too.[20] Lanthanide ions with their large coordination numbers are useful in generation of new and unusual network topologies.[21]

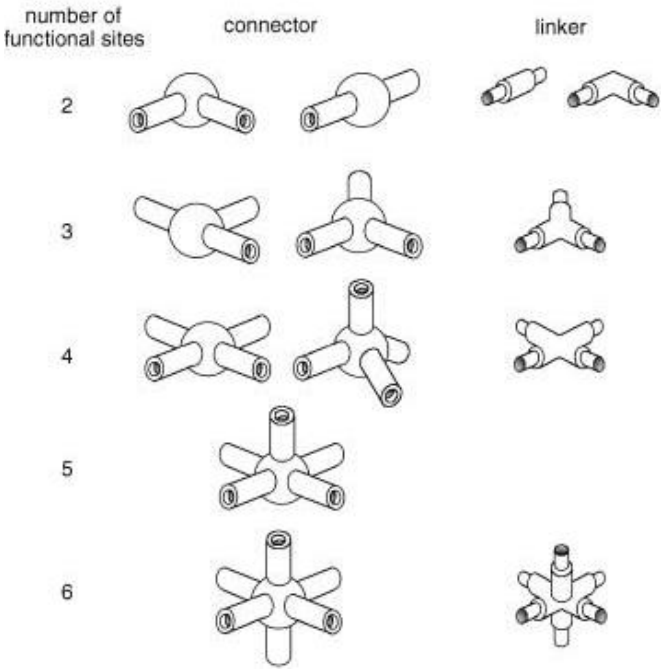

Figure 1. Various connector and ligand/linker geometries. Adapted from Reference 19.

Organic ligands/linkers with rigid backbones are often preferred, because the rigidity makes it easier to predict the network geometry in advance of synthesis, and helps in sustaining the open pore structure after the removal of the included solvent. These can be electrically neutral, anionic, or cationic (Figure 2). Currently, multidentate nitrogen- and oxygen-donor organic ligands are preferred in the synthesis of MOCNs due to their thermal stability and possible prevention of structural collapse after removal of guest molecules. The commonly used neutral organic ligands/linkers are pyrazine and 4,4'-bipyridine (4,4'-bpy), useful as pillars in the

construction of pillared layer in 3D networks.[22,23] Anionic ligands/linkers are mostly carboxylates[24] due to their ability to aggregate metal ions into clusters thereby forming more stable frameworks. Cationic ligands/linkers, such as pyridinium salts, are little used due to their low affinities for cationic metal ions.[25]

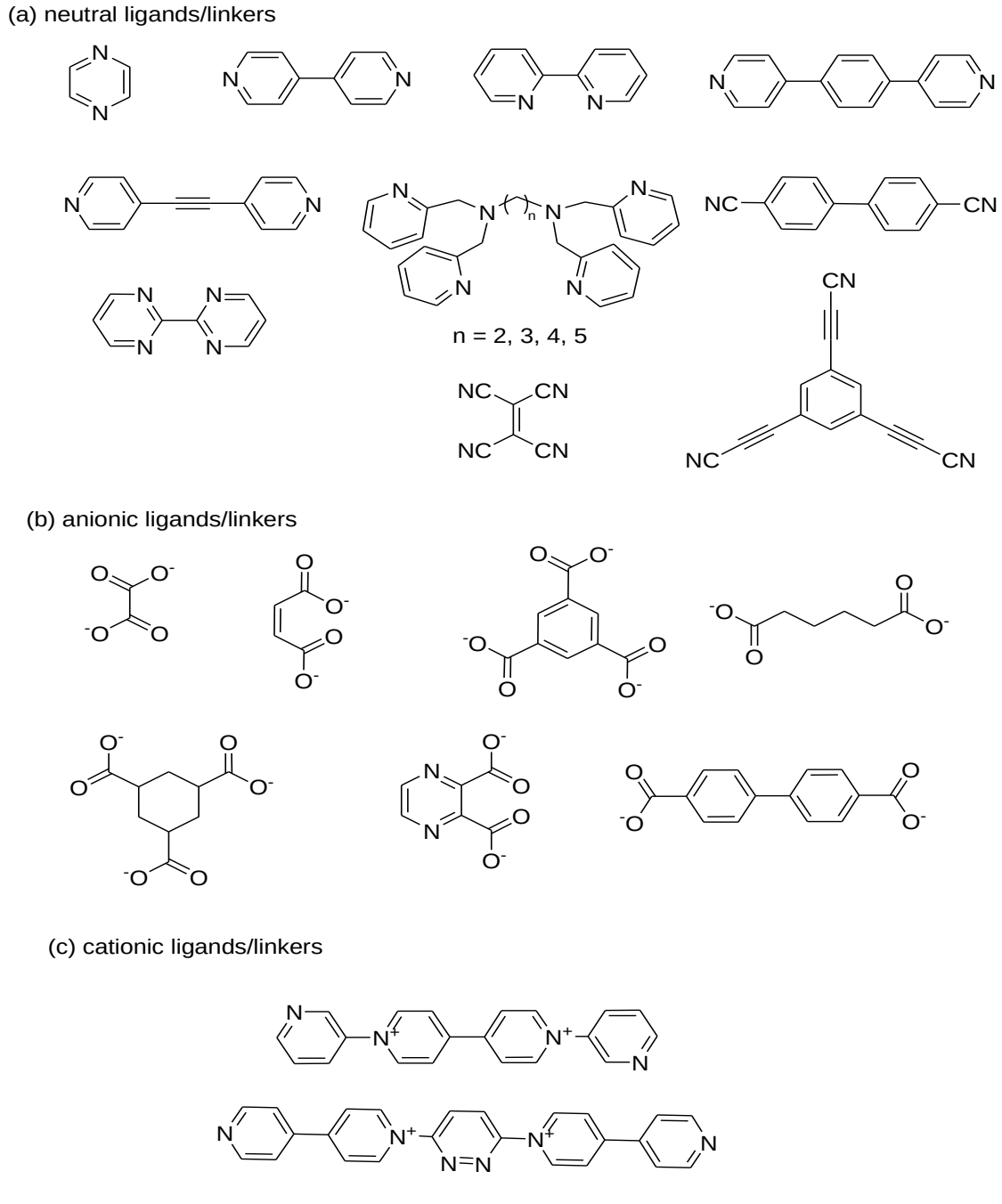

Figure 2. Examples of ligands and linkers. Adapted from references 19 and 17b.

Specific structural motifs can be obtained using various combinations of the connectors and the ligands/linkers mentioned above (Figure 3). Generally, metal ions having higher coordination number tend to generate 3-dimensional structures, while those with the lower coordination number tend to generate 1- and 2-dimensional structures.

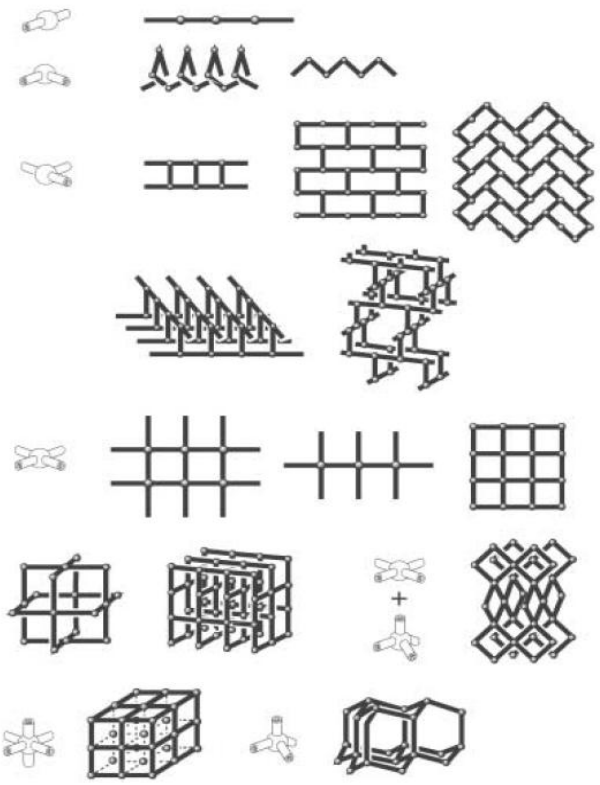

Figure 3. Possible frameworks resulting from combination of connectors and ligands/linkers. Adapted from Reference 19.

MOCNs can be synthesized by a variety of methods such as conventional one-pot synthesis, solvothermal/hydrothermal synthesis, microwave-assisted, sonochemical, electrochemical, mechanochemical, ionothermal, dry-gel conversion, and microfluidic synthesis.[26]

The conventional one-pot synthesis includes mixing of the starting materials in a solvent, at room temperature or elevated temperatures, resulting in precipitation followed by recrystallization or slow evaporation of the solvent. Methods such as solvent evaporation of a solution of reactants, layering of solutions, or slow diffusion of reactants into each other lead to concentration gradients that can generate MOCNs. HKUST-1 and ZIF-8 are few examples of

networks obtained through this procedure.[27] The other synthesis techniques are outlined in Schemes 1 and 2.

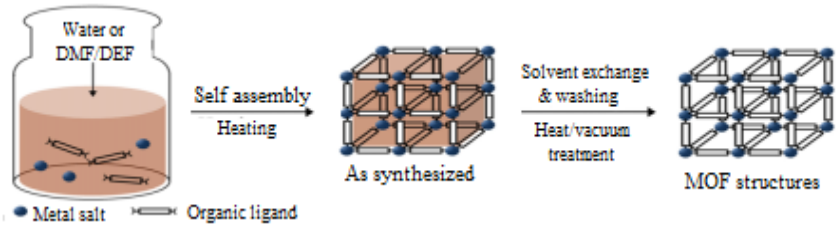

(i)

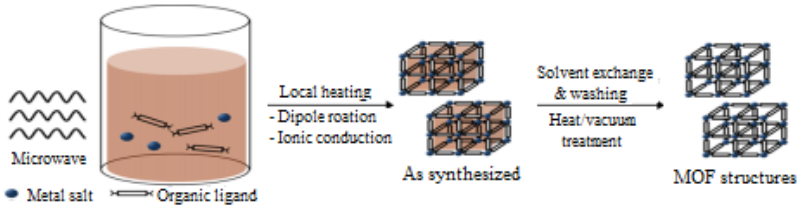

(ii)

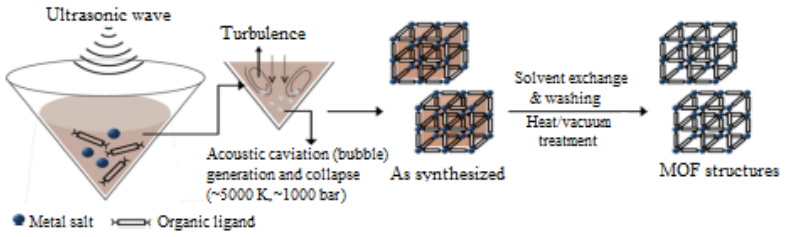

(iii)

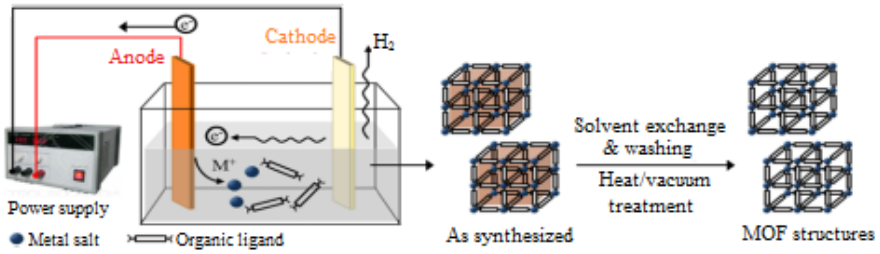

(iv)

Scheme 1. Depiction of (i) conventional solvothermal synthesis; (ii) microwave assisted solvothermal synthesis; (iii) sonochemical synthesis; (iv) electrochemical synthesis. Adapted from Reference 26.

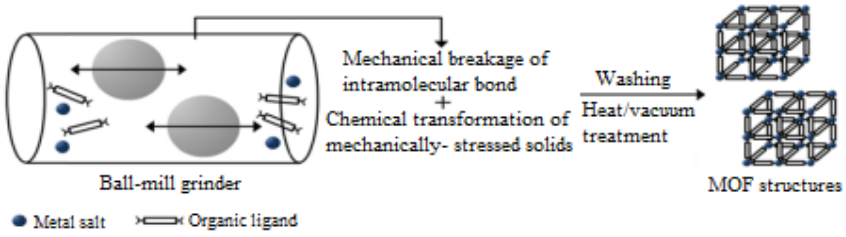

(v)

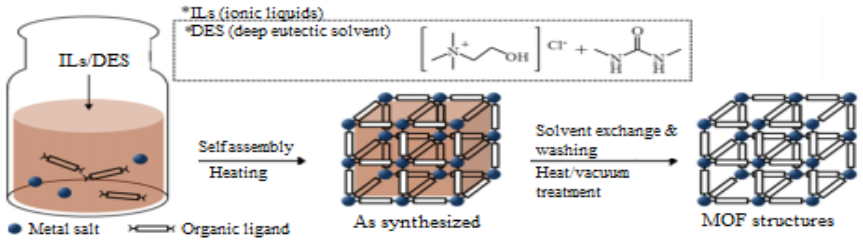

(vi)

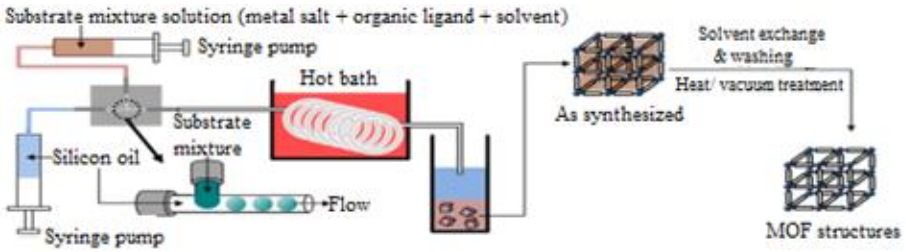

(vii)

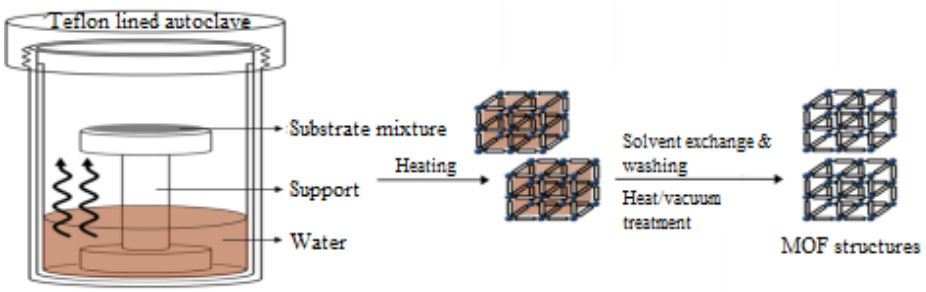

(viii)

Scheme 2. Other synthesis techniques: (v) mechanochemical synthesis; (vi) ionothermal synthesis; (vii) microfluidics synthesis; and (viii) dry gel conversion synthesis. Adapted from Reference 26.

Applications of MOCNs

MOCNs have attracted a wide interest because these provide a novel route towards porous materials that may find applications in gas storage, adsorption based gas/vapor separation, shape/size-selective catalysis, drug storage and delivery, and as templates in the preparation of low dimensional materials.[28]

Gas storage

A key challenge faced in the world today is the ever growing energy demand and the depletion of non-renewable energy sources. Hydrogen is a promising candidate in the alternative energy arena and an ideal energy carrier due to its zero carbon content, and its high gravimetric energy density, which can nearly triple that of gasoline. Moreover, hydrogen can be generated from an almost inexhaustible resource - water. One of the biggest bottlenecks to realizing a hydrogen economy is the lack of a safe, efficient, and economical on-board hydrogen storage system.

In 2003, Rosi et al. reported the first MOF-based hydrogen storage study.[29] Subsequently, more than 150 MOFs have been tested for their hydrogen uptake capacity.[30] So far, the highest excess gravimetric uptake at saturation is held by MOF-177, which demonstrates an excess uptake capacity of 0.076 kg/kg at 77 K and 70 bar corresponding to a record absolute value of 0.112 kg/kg, and this can be ascribed to its exceptionally high surface area of 5600 m^2/g.[31]

Great efforts have been dedicated to the exploration of various strategies to enhance hydrogen uptake in porous MOFs at 77 K and 1 atm, and these studies can be very useful and instructive at this early stage of exploration for hydrogen storage materials. The major hurdle limiting hydrogen uptake at ambient temperature is the weak interaction between hydrogen molecules and the frameworks of porous MOFs.

Methane storage[32] and carbon dioxide capture by MOFs are also being intensively studied. PCN-14, which contains copper(II) ions and 5,5'-(9,10-anthracenediyl)di-isophthalate units, shows highest methane adsorption capacity: 230 v/v at 290 K and 35 bar.[33]

Carbon dioxide uptake has also been tested in other MOFs and can be greatly improved if pendant alkylamine functional groups are introduced into the pore surface.

Selective gas adsorption

The principal mechanisms based on which selective gas adsorption is achieved in MOFs are adsorbate–surface interactions and size-exclusion (molecular sieving effect). The former involves the chemical and/or physical interaction between the adsorbent and the adsorbate while the latter depends on the dimension and shape of the framework pores. These two effects are capable of working independently as well as cooperatively.

MOFs have been incorporated into thin-film materials to aid in gas separation. The copper net supported $Cu_3(btc)_2$ MOF thin film developed by Guo et al. demonstrated the successful separation of H_2 from H_2/N_2, H_2/CO_2, and H_2/CH_4 mixtures. This MOF demonstrated excellent permeation selectivity for H_2 and possessed separation factors much higher than traditional zeolites.[34]

Catalysis

As porous materials, MOFs may prove to be very useful in catalysis. Theoretically, the pores of MOFs can be tailored in a systematic way allowing optimization for specific catalytic applications. Besides the high metal content of MOFs, one of their greatest advantages is that the active sites are rarely different because of the highly crystalline nature of the material. Although catalysis is one of the most promising applications of such materials, only a few examples have been reported to date. In these MOFs, size- and shape-selective catalytic applications depend on porosity and the presence of catalytically active transition metal centers. Gándara et al. obtained a new In(III) MOF composed of thick layers containing square-shaped channels. The channels are empty in In(OH)L and filled with pyridine in [In(OH)L]·xPy (L = 4,4-(hexafluoroisopropylidene)bis(benzoate)). This microporous, thermally stable compound has been proven to be an efficient heterogeneous catalyst for acetalization of aldehydes.[35]

Drug Delivery

The inability of conventional orally administered drugs to deliver medication at a controlled release rate has spawned much interest and research in novel methods for drug delivery. Organic systems benefit from a wide array of biocompatibility, the ability to uptake many drugs, yet lack a controlled release mechanism. The inorganic delivery materials are able to deliver the adsorbed

drugs at a controlled rate due to their ordered porous network, but have a decreased loading capacity. Loiseau et al. studied the drug-delivery rate of MIL-53, a flexible material known for its ability to expand its structure upon heating in what is termed a breathing effect. MIL-53, with a maximum volume of approximately 1500 $Å^3$ at high temperature and full expansion, was able to uptake approximately 20 wt% of ibuprofen with a complete delivery taking approximately three weeks.[36] The long, steady delivery can be attributed to the flexibility of the framework to bend around the ibuprofen molecules to maximize the bonding interactions while still minimizing steric hindrance. Although progress has been made, and MOFs have proven themselves suitable candidates for drug delivery, much research needs to be done to realize the full potential of MOFs as materials for drug delivery.

As templates for synthesis of low dimensional materials

The construction of complex assemblies using molecular building blocks is paramount for the development of novel functional materials. Through the use of transition-metal centers and concepts from coordination chemistry, a rich variety of molecular nanostructures and architectures with well-defined shapes and geometries have been obtained. The controlled nanoscale fabrication of functional molecular architectures at well-defined substrates is desirable for many applications. Two-dimensional (2D) supramolecular coordination networks assembled directly at surfaces can be viewed as analogues of the three-dimensional (3D) MOFs. As these are formed on solid substrates, the structures of these 2D networks and the self-assembly processes can be monitored in single molecule detail using advanced surface science techniques like scanning tunneling microscopy (STM).[37]

The sequential deposition of 1,2,4-benzenetricarboxylic acid (trimellitic acid, tmla) molecules and Fe atoms on a clean Cu(100) substrate under UHV conditions gives rise to the formation of 2D surface-supported open networks, stabilized by strong lateral metal-organic coordination bonds. The subtle variation of the relative quantities of the constituents that are deposited can steer the modular assembly of distinct metal-carboxylate network architectures. This approach opens novel avenues for the fabrication of nanoscale functional materials.[38]

Present work

The use of a multidentate ligand along with a multiatom carboxylate linker has been an effective design strategy in the synthesis of MOCNs, as it not only provides a variety of network assemblies and interesting topologies, but also allows for tenability in the pore sizes.

A large number of MOCNs have been synthesized using bidentate, tridentate and tetradentate ligands; but only a few using penta or hexadentate ligands are reported.

A hexadentate ancillary ligand, N,N',N'',N'''-tetrakis-(2-pyridylmethyl)-1,4-diaminobutane (tpbn), is known in the literature for a variety of applications. Tetranuclear μ-oxo-bis(μ-carboxylato)-bridged Fe^{III} complexes with tpbn similar to met forms of hemerythrin[39,40] and a dimeric vanadium complex of bioinorganic relevance are reported.[41] A series of bridging ligands containing the two dipicolylamine moieties have further been used to control the thermodynamic and kinetic properties of transition-metal complexes and several bridged Pt(II) complexes which typically work as DNA-binding reagents, the bioactivities of which are adjusted by the nature of the bridging ligands and having potential anti-tumor activities are there in the literature.[42,43] However, for the first time Khullar et al. utilized a series of hexadentate polypyridyl ancillary ligands differing in methylene chain lengths between the alkyl nitrogens to make diverse MOCNs including a 3D MOCN of tpbn held together by strong hydrogen bonding and π−π interactions.[17b]

In this work, an attempt was made to study a variation in the position of nitrogen donor atoms on the pyridyl rings. A change in the nitrogen position can have a remarkable effect on the geometry of the ligand and subsequently on coordination to the metal ion and the network structure. Two new derivatives of tpbn, N, N', N'', N'''-tetrakis-(4-pyridylmethyl)-1,4-diaminobutane (4-pytpbn) and N, N"-bis-(2-pyridylmethyl)-N', N'''-bis-(4-pyridylmethyl)-1,4-diaminobutane (2,4-pytpbn) were synthesized (Figure 4). Metal ions, such as Co(II), Ni(II), Cu(II), Zn(II) and Cd(II), were used in the synthesis of complexes. The linkers used were acetylenedicarboxylate (adc), fumarate (fum) and succinate (succ), as shown in Figure 5.

All complexes were characterized by elemental analysis, FTIR spectroscopy, thermogravimetric analysis (TGA) and powder X-ray diffraction (PXRD).

Figure 4. Ancillary ligands made for this study.

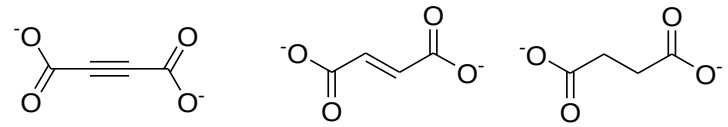

Figure 5. Linkers used in this study.

Chapter II

Experimental Section

Materials and Methods

All chemicals and solvents used for synthesis were obtained from commercial sources and used as received without further purification. Dry solvents were obtained from mBRAUN MB SPS 800 solvent purification system. Elemental analysis (CHN) was carried out at NIPER Mohali. The ^{1}H NMR spectra of the ligands were obtained in $CDCl_3$ solution at 25 ˚C on a Bruker ARX-400 spectrometer; chemical shifts are reported relative to the residual solvent signals. Thermogravimetric analysis (TGA) was carried out from 25 to 500 °C (at a heating rate of 10 °C/min) under dinitrogen atmosphere on a Shimadzu DTG-60H analyser. FTIR spectra were recorded for solid samples prepared as KBr pellets and liquid samples on KCl plates in the 400-4000 cm^{-1} range on a Perkin-Elmer Spectrum One spectrophotometer with a resolution of 4 cm^{-1}. Single crystal and powder X-ray diffraction studies were carried on a Bruker Kappa Apex II diffractometer and a Rigaku Ultima IV diffractometer, respectively, located in the X-ray facility of IISER Mohali.

Caution! Perchlorates were used as the metal salts in this study. Since these are explosive, proper care should be taken while handling these metal salts.

Synthesis of Ligands

4-pytpbn.[44] In a 50 ml Schlenck flask a mixture of 1,4-diaminobutane (0.6 mL, 6 mmol) and 4-pyridinecarboxaldehyde (2.7 mL, 29 mmol) was prepared in 8 mL of 1,2-dichloroethane (DCE) and stirred for 4 h at room temperature under a dinitrogen atmosphere. Sodium triacetoxyborohydride (6 g, 29 mmol) was added in two portions (5.2 g + 0.8 g) at an interval of 24 h along with an additional 15 ml DCE and the solution was stirred for 48 h at room temperature under a dinitrogen atmosphere yielding a reddish brown solution. After neutralization with saturated aqueous $NaHCO_3$ (25 mL) to give a weakly alkaline solution, the product was extracted with chloroform and dried over anhydrous sodium sulfate. The crude solid obtained by evaporation of the solvent under reduced pressure was washed with diethylether and dissolved in minimum amount of ethyl acetate for crystallization. After a few days, colorless

crystals of 4-pytpbn were obtained. Yield: 1.28 g (48%). Selected FTIR peaks (KBr, cm^{-1}): 3421 (br), 2817 (w), 1601 (s), 1560 (m), 1413 (s), 1119 (m), 798 (s), 786 (m), 624 (w), 473 (w). ^1H NMR ($CDCl_3$, δ, ppm): 1.16 (4H, q, J = 4 Hz), 2.36 (4H, t, J = 6 Hz), 3.55 (8H, s), 7.30 (8H, d, J = 6 Hz), 8.56 (8H, dd, J = 2.4 Hz).

2,4-pytpbn. Step 1: To a solution of 1,4-diaminobutane (1 ml, 10 mmol) in 2 ml methanol, 4-pyridinecarboxaldehyde (2 mL, 20 mmol) was added in a 10 mL RB flask and stirred for 4 h at room temperature under a dinitrogen atmosphere. To the product obtained, sodium borohydride (760 mg, 20 mmol) was added over 15 minutes at 0 ˚C and the mixture was stirred for another 24 h at room temperature under a dinitrogen atmosphere. The resulting solution was extracted with chloroform and dried over anhydrous sodium sulphate. The reduced Schiff base was obtained by removal of solvent under reduced pressure as a yellow oily liquid which solidified upon cooling. Yield: 1.73g (67 %). Step 2: In a 25 mL RB flask, 4-pybn (300 mg, 1 mmol) that was obtained in step 1 and picolylchloride hydrochloride (364 mg, 2 mmol) were mixed in 5 mL water followed by the addition of an aqueous solution of sodium hydroxide (178 mg, 8.75 mmol in 2 mL water). The contents were stirred for 24 h at room temperature and the resulting mixture was extracted with chloroform. The crude product obtained was purified by column chromatography using a mixture of ethyl acetate and methanol (20:1). Upon evaporation of solvents under reduced pressure, colorless crystals of 2,4-pytpbn were obtained. Yield: 103 mg (20%). Selected FTIR peaks (KBr, cm^{-1}): 3402 (br), 2808 (w), 1596 (s), 1433 (s), 1412 (s), 1122 (m), 796 (s), 764 (s), 614 (m), 471 (w). ^1H NMR ($CDCl_3$, δ, ppm): 1.53 (4H, q, J = 3 Hz), 2.45 (4H, t, J = 6 Hz), 3.62 (4H, s), 3.74 (4H, s) 7.17 (2 H, t, J = 6Hz), 7.30 (4H, d, J = 2Hz), 7.47 (2H, d, J = 4Hz), 7.66 (2H, t, J = 8 Hz), 8.52 (6H, dd, J = 2 Hz).

Synthesis of Metal Complexes

The metal complexes were synthesized via the following methodologies:

Method 1: To a methanolic solution (4.5 ml) of $MX_2{\cdot}nH_2O$ (0.2 mmol), 4-pytpbn (0.2 mmol) was added and the reaction mixture either refluxed at 80 ˚C or stirred at room temperature for 4h. The resulting solution was filtered, washed with methanol and air-dried to obtain the product.

Method II: To a methanolic solution (4 ml) of $M(OAc)_2{\cdot}nH_2O$ (0.125 mmol), 4-pytpbn (0.0625 mmol) was added followed by the respective dicarboxylic acid (0.0125 mmol) and the reaction

mixture was stirred for 4 h at room temperature. Upon removal of the solvent under reduced pressure, the solid obtained was treated with a mixture of toluene and acetonitrile (1:1 v/v) to get rid off the acetic acid and air-dried.

The following compounds were synthesized by **Method I:**

{[Co(4-pytpbn)Cl_2]·H_2O}$_n$ (1). $CoCl_2 \cdot 6H_2O$ was used as the metal salt. Dry methanol was used. The mixture was refluxed. A blue solid was obtained. Yield (%): 82. Selected FTIR peaks (KBr, cm^{-1}): 3434 (br), 2930 (w), 1615 (s), 1561 (m), 1425 (m), 1368 (w), 1226 (m), 1063 (m), 1017 (m), 817 (m), 632 (m), 531 (w). Anal. Calcd. for $C_{28}H_{34}N_6OCl_2Co$: C, 55.99; H, 5.70; N, 13.98. Found: C, 56.37; H, 5.40; N, 13.74. Single crystals suitable for X-ray diffraction studies were grown by direct layering of the reactants.

{[Co(4-pytpbn)$(NO_3)_2$]·$6H_2O$}$_n$ (2). $Co(NO_3)_2 \cdot 6H_2O$ was used as the metal salt. The mixture was refluxed. Light pink solid was obtained. Yield (%): 76. Selected FTIR peaks (KBr, cm^{-1}): 3399 (br), 2942 (w), 1616 (s), 1560 (s), 1421 (s), 1384 (s), 1231 (m), 1062 (m), 1019 (m), 816 (m), 726 (w), 635 (m), 487 (w). Anal. Calcd for $C_{28}H_{44}N_8O_{12}Co$: C, 45.22; H, 5.92; N, 15.07. Found: C, 45.35; H, 4.81; N, 15.00. Single crystals suitable for X-ray diffraction studies were grown by direct layering of the reactants.

{[Cd(4-pytpbn)$(NO_3)_2$]·H_2O}$_n$ (3). $Cd(NO_3)_2 \cdot 4H_2O$ was used as the metal salt. The mixture was stirred. A pale yellow solid was obtained. Yield (%): 88. Selected FTIR peaks (KBr, cm^{-1}): 3422 (br), 1612 (m), 1425 (m), 1384 (s), 1297 (b), 1225 (w), 1062 (w), 1018 (w), 811 (m). Anal. Calcd for $C_{28}H_{34}N_8O_7Cd$: C, 47.56; H, 4.84; N, 15.84. Found: C, 48.10; H, 4.70; N, 15.40.

{[Cu(4-pytpbn)$(NO_3)_2$]·$5H_2O$}$_n$ (4). $Cu(NO_3)_2 \cdot 3H_2O$ was used as the metal salt. The mixture was stirred. A dark blue solid was obtained. Yield (%): 89. Selected FTIR peaks (KBr, cm^{-1}): 3399 (br), 2935 (w), 2812 (w), 1618 (m), 1560 (m), 1428 (w), 1384 (s), 1226 (w), 1130 (w), 1060 (m), 1030 (m), 814 (m). Anal. Calcd. for $C_{28}H_{42}N_8O_{11}Cu$: C, 46.05; H, 5.75; N, 15.35. Found: C, 46.09; H, 5.54; N, 14.73.

{[Co(4-pytpbn)$(CH_3OH)_2$]$(ClO_4)_2$·$6H_2O$}$_n$ (5). $Co(ClO_4)_2 \cdot 6H_2O$ was used as the metal salt. The mixture was refluxed. A pink solid was obtained. Yield (%): 70. Selected FTIR peaks (KBr, cm^{-1}): 3434 (br), 2930 (w), 1615 (s), 1561 (m), 1425 (m), 1368 (w), 1226 (m) , 1063 (m), 1017 (m),

817 (m), 632 (m), 531 (w). Anal. Calcd for $C_{30}H_{52}N_6Cl_2O_{16}Co$: C, 40.82; H, 5.89; N, 9.52. Found: C, 40.90; H, 5.19; N, 9.69.

The following compounds were synthesized by **Method II:**

{[$Zn_2(adc)_2(4\text{-}pytpbn)$]·$6H_2O$}$_n$ (6). $Zn(OAc)_2{\cdot}2H_2O$ and acetylenedicarboxylic acid were used as the metal salt and the dicarboxylic acid, respectively. A light brown solid was obtained. Yield (%): 88. Selected FTIR peaks (KBr, cm^{-1}): 3422 (br), 1636 (m), 1618 (s), 1430 (m), 1332 (b), 1226 (w), 774 (m), 690 (m). Anal. Calcd. for $C_{36}H_{48}N_6O_{14}Zn_2$: C, 47.22; H, 4.80; N, 9.18. Found: C, 47.00; H, 4.47; N, 10.35.

{[$Cd_2(adc)_2(4\text{-}pytpbn)$]·$4H_2O$}$_n$ (7). $Cd(OAc)_2{\cdot}2H_2O$ and acetylenedicarboxylic acid were used as the metal salt and the dicarboxylic acid, respectively. A light brown solid was obtained. Yield (%): 65. Selected FTIR peaks (KBr, cm^{-1}): 3422 (br), 1616 (s), 1590 (w), 1425 (m), 1364 (m), 1330 (m), 780 (w), 674 (w). Anal. Calcd. for $C_{36}H_{40}N_6O_{12}Cd_2$: C, 44.40; H, 4.11; N, 8.63. Found: C, 44.75; H, 4.04; N, 7.87.

{[$Ni_2(fum)_2(4\text{-}pytpbn)$]·$6H_2O$}$_n$ (8). $Ni(OAc)_2{\cdot}4H_2O$ and fumaric acid (fum) were used as the metal salt and the dicarboxylic acid, respectively. A dark green solid was obtained. Yield (%): 74. Selected FTIR peaks (KBr, cm^{-1}): 3377 (br), 2935 (w), 1708 (w), 1615 (s), 1557 (s), 1425 (m), 1384 (s), 1278 (w), 1224 (w), 1063(w), 1024 (m), 982 (m), 806 (m), 679 (m). Anal. Calcd. for $C_{36}H_{46}N_6O_{14}Ni_2$: C, 47.71; H, 5.30; N, 9.27. Found: C, 46.20; H, 5.35; N, 7.77.

{[$Ni_2(succ)_2(4\text{-}pytpbn)$]·$4H_2O$·$3CH_3OH$}$_n$ (9). $Ni(OAc)_2{\cdot}4H_2O$ and succinic acid (succ) were used as the metal salt and the dicarboxylic acid, respectively. A light green solid was obtained. Yield (%): 88. Selected FTIR peaks (KBr, cm^{-1}): 3391 (br), 3072 (w), 2933 (w), 1716 (w), 1616 (s), 1560 (s), 1425 (s), 1063 (m), 1023 (m), 814 (m), 733 (w), 666 (m), 620 (m). Anal. Calcd. for $C_{39}H_{60}N_6O_{15}Ni$: C, 48.64; H, 5.97; N, 8.96. Found: C, 48.37; H, 5.80; N, 8.37.

Single Crystal X-ray Studies

Crystals of the compounds were transferred from mother liquor to mineral oil for manipulation, selection, and mounting in a nylon loop attached to a goniometer head. Initial crystal evaluation and data collection were performed on a Kappa APEX II diffractometer equipped with a CCD detector (with the crystal-to-detector distance fixed at 60 mm) and sealed-tube monochromated

Mo Kα radiation. The diffractometer was interfaced to a PC that controlled the crystal centering, unit cell determination, refinement of the cell parameters, and data collection through the program APEX2.[45] For each sample, three sets of frames of data were collected with 0.30° steps in ω and an exposure time of 10 s within a randomly oriented region of reciprocal space surveyed to the extent of 1.3 hemispheres to a resolution of 0.85 Å. By using the program SAINT[45] for the integration of the data, reflection profiles were fitted, and values of F^2 and $\sigma(F^2)$ for each reflection were obtained. Data were also corrected for Lorentz and polarization effects. The subroutine XPREP[45] was used for the processing of data that included determination of space group, application of an absorption correction (SADABS),[45] merging of data, and generation of files necessary for solution and refinement. The crystal structures were solved and refined using SHELX 97.[46] Positions of most of the non hydrogen atoms were obtained from a direct methods solution. Several full-matrix least-squares/difference Fourier cycles were performed, locating the remainder of the non-hydrogen atoms. All non-hydrogen atoms, except where indicated otherwise, were refined with anisotropic displacement parameters. All hydrogen atoms were placed in ideal positions and refined as riding atoms with individual isotropic displacement parameters. Crystallographic parameters and basic information pertaining to data collection and structure refinement for 4-pytpbn and 2,4-pytpbn are summarized in Table 3. All figures were drawn using Mercury V 3.0,[47] and hydrogen bonding parameters were generated using Platon[48].

Powder X-ray Studies

PXRD data were recorded on a Rigaku Ultima IV diffractometer equipped with a 3 KW sealed tube Cu KαX-ray radiation (generator power settings: 40 kV and 40 mA) and a DTex Ultra detector using parallel beam geometry (2.5° primary and secondary solar slits, 0.5° divergence slit with 10 mm height limit slit). Each sample grounded into a fine powder using a mortar and a pestle was placed on a glass sample holder that was placed on the sample rotation stage (120 rpm) attachment. The data were collected over an angle range 5° to 50° with a scanning speed of 2° per minute with 0.02° step with XRF reduction for metal complexes.

Chapter III

Results and Discussion

Synthesis

The aim of this study was to synthesize MOCNs based on multidentate ligands. Supramolecular assemblies and networks based on polypyridyl ligand N,N',N",N'''-tetrakis-(2-pyridylmethyl)-1,4-diaminobutane (tpbn) have already been reported.[17b] This work was in continuation of the previous work on tpbn. Thus, two new ancillary ligands, N, N', N", N'''-tetrakis-(4-pyridylmethyl)-1,4-diaminobutane (4-pytpbn) and N, N''-bis-(2-pyridylmethyl)-N', N'''-bis-(4-pyridylmethyl)-1,4-diaminobutane (2,4-pytpbn) were synthesized as shown in Schemes 3 and 4.

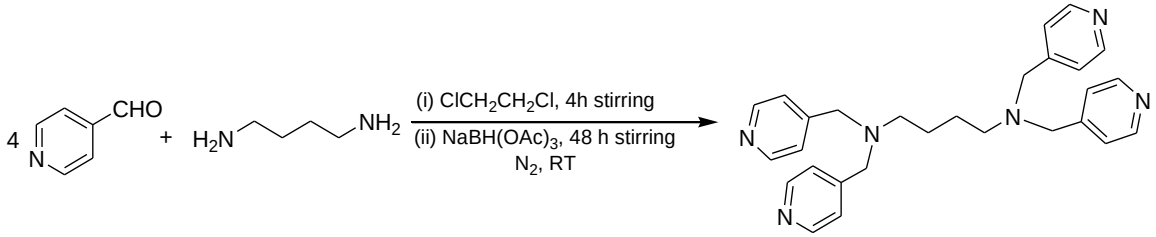

Scheme 3. Synthesis of 4-pytpbn.

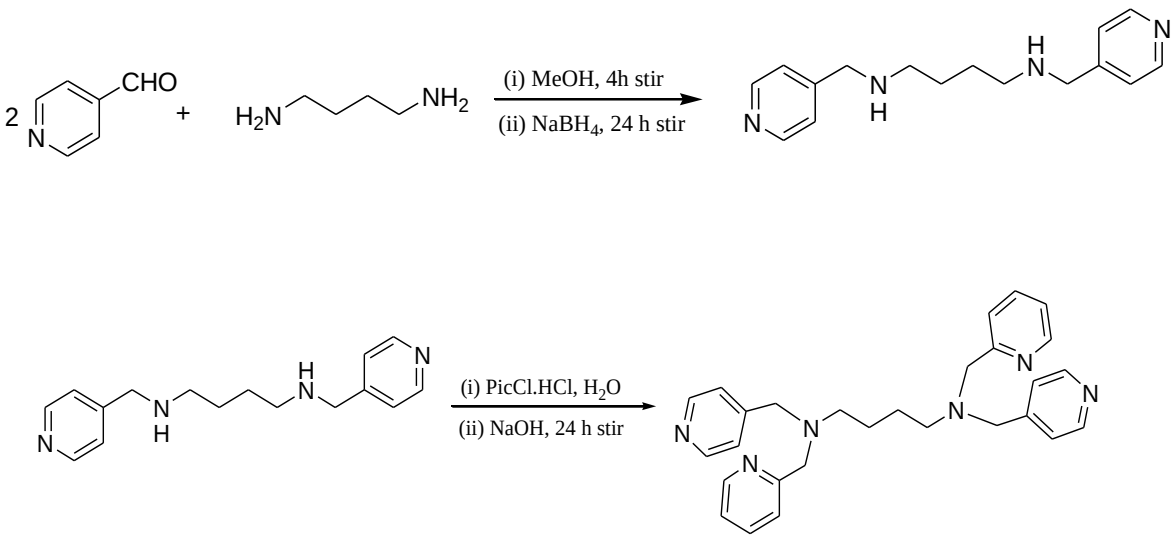

Scheme 4. Synthesis of 2,4-pytpbn.

Metal complexes **1**-**9** were synthesized as shown in Scheme 5. Complexes **1**, **2** and **5** are soluble in methanol/water, methanol/acetonitrile mixtures and DMSO. Rest of the complexes (**3, 4, 6**, **7** and **8**) are insoluble in common organic solvents. Complexes **1** and **5** are light pink, **2** and **4** are blue, **3** is light yellow, **6** and **7** are light white-brown, and **8** and **9** are green.

$$CoCl_2{\cdot}6H_2O + \text{4-pytpbn} \xrightarrow[4\text{ h, }80\ ^oC]{\text{MeOH}} \{[Co(\text{4-pytpbn})Cl_2]{\cdot}5H_2O\}_n\ (\mathbf{1})$$

$$Co(NO_3)_2{\cdot}6H_2O + \text{4-pytpbn} \xrightarrow[4\text{ h, }80\ ^oC]{\text{MeOH}} \{[Co(\text{4-pytpbn})(NO_3)_2]{\cdot}6H_2O\}_n\ (\mathbf{2})$$

$$Cd(NO_3)_2{\cdot}4H_2O + \text{4-pytpbn} \xrightarrow[4\text{ h, stir}]{\text{MeOH}} \{[Cd(\text{4-pytpbn})(NO_3)_2]{\cdot}H_2O\}_n\ (\mathbf{3})$$

$$Cu(NO_3)_2{\cdot}3H_2O + \text{4-pytpbn} \xrightarrow[4\text{ h, stir}]{\text{MeOH}} \{[Cu(\text{4-pytpbn})(NO_3)_2]{\cdot}5H_2O\}_n\ (\mathbf{4})$$

$$Co(ClO_4)_2{\cdot}6H_2O + \text{4-pytpbn} \xrightarrow[4\text{ h, }80\ ^oC]{\text{MeOH}} \{[Co(\text{4-pytpbn})(CH_3OH)_2](ClO_4)_2{\cdot}6H_2O\}_n\ (\mathbf{5})$$

$$2\ Zn(OAc)_2{\cdot}2H_2O + \text{4-pytpbn} + 2\ H_2\text{adc} \xrightarrow[4\text{ h, stir}]{\text{MeOH}} \{[Zn_2(\text{adc})_2(\text{4-pytpbn})]{\cdot}6H_2O\}_n\ (\mathbf{6})$$

$$2\ Cd(OAc)_2{\cdot}2H_2O + \text{4-pytpbn} + 2\ H_2\text{adc} \xrightarrow[4\text{ h, stir}]{\text{MeOH}} \{[Cd_2(\text{adc})_2(\text{4-pytpbn})]{\cdot}4H_2O\}_n\ (\mathbf{7})$$

$$2\ Ni(OAc)_2{\cdot}4H_2O + \text{4-pytpbn} + 2\ H_2\text{fum} \xrightarrow[4\text{ h, stir}]{\text{MeOH}} \{[Ni_2(\text{fum})_2(\text{4-pytpbn})]{\cdot}6H_2O\}_n\ (\mathbf{8})$$

$$2\ Ni(OAc)_2{\cdot}4H_2O + \text{4-pytpbn} + 2\ H_2\text{succ} \xrightarrow[4\text{ h, stir}]{\text{MeOH}} \{[Ni_2(\text{succ})_2(\text{4-pytpbn})]{\cdot}4H_2O{\cdot}3CH_3OH\}_n\ (\mathbf{9})$$

Scheme 5. Synthesis of metal complexes with 4-pytpbn.

NMR Spectroscopy

The ^{1}H NMR spectra of 4-pytpbn and 2,4-pytpbn are shown in Figures 6 and 7, respectively. While the pure product is confirmed for 4-pytpbn, the presence of the desired product along with some impurities is observed for 2,4-pytpbn. The ^{1}H NMR of 4-pytpbn shows a quintet at 1.16 ppm (4H) and a triplet at 2.36 ppm (4H) for the butane chain, a singlet at 3.55 ppm (8H) for the –CH_2 group of the pyridyl groups. Due to the symmetry of the molecule, in the aromatic region only two sets of protons appear at 7.30 ppm (8H) as a doublet and at 8.56 ppm (8H) as a double of doublet.

For 2,4-pytpbn, the quintet and triplet of the butane chain appear at 1.53 ppm (4H) and 2.45 ppm (4H), singlets of the -CH_2 group of the 2-py and 4-py groups appear at 3.62 (4H) and 3.74 ppm (4H), respectively. Protons corresponding to the aromatic rings appear as three doublets at 7.30 ppm (4H), 7.47 ppm (2H), two triplets at 7.17 ppm (2H) and 7.66 ppm (2H) and adouble of doublet at 8.52 ppm (6H).

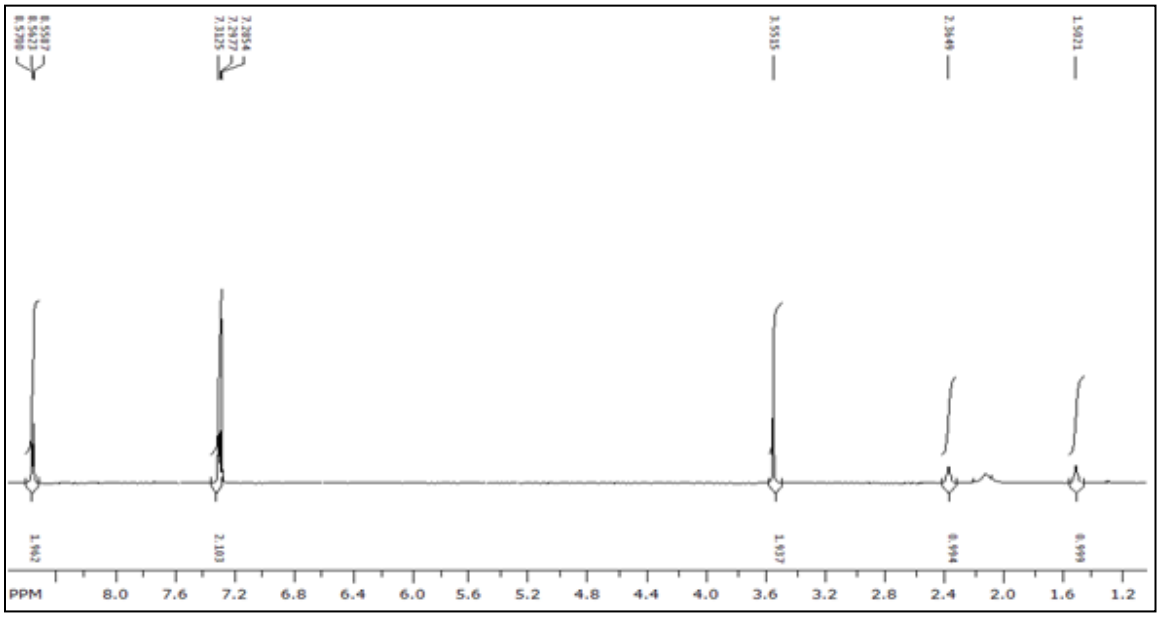

Figure 6. ^{1}H NMR spectrum of 4-pytpbn.

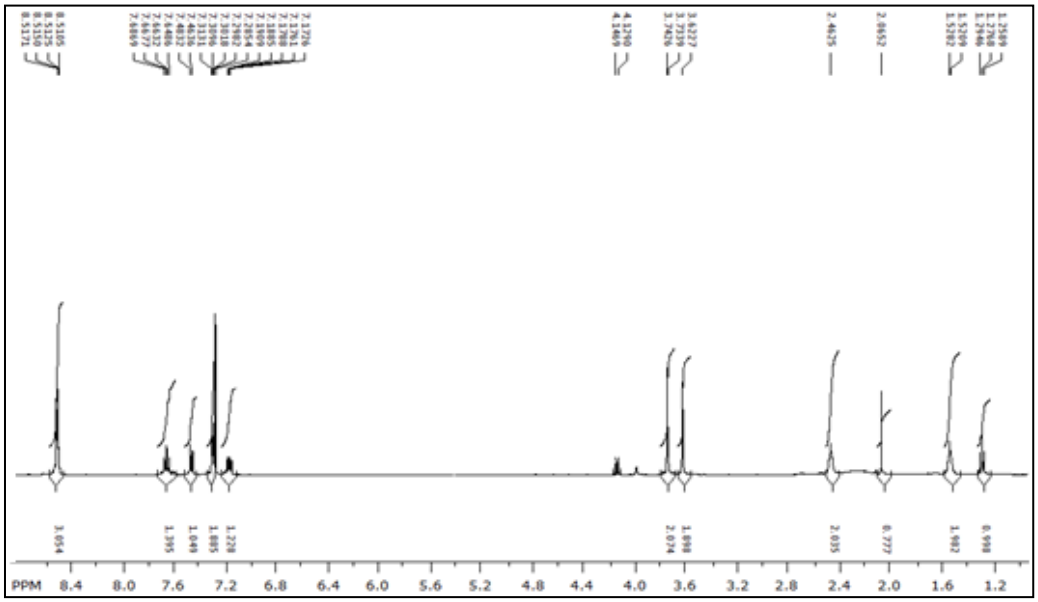

Figure 7. ^{1}H NMR spectrum of 2,4-pytpbn.

FTIR Spectroscopy

The IR spectra of all complexes (**1-9**) recorded in the solid state show a broad band centered at 3400 cm^{-1} which is a characteristic feature for O-H stretching frequency of water molecules. A Peaks around 3240 cm^{-1} in a few of these complexes shows the presence of lattice water. Peaks centered around 1615 cm^{-1}, 1475 cm^{-1} and 815 cm^{-1} are due to the ligand. The nitrate stretching frequencies occur at 1384 cm^{-1}, 1297 cm^{-1} and 1018 cm^{-1} for the monodentate binding mode; and at 1425 cm^{-1}, 1225 cm^{-1} and 1062 cm^{-1} for binding in a chelating bidentate fashion. The $\Delta\nu$ values (the difference between the asymmetric and symmetric stretching frequencies of the carboxylate groups) of 286 and 252 cm^{-1} for complexes **6** and **7**, respectively, correspond to a monodentate binding mode. For complexes **7** and **8**, the $\Delta\nu$ values are 173 and 136 cm^{-1}, respectively, indicating a chelating bidentate mode. The perchlorate stretching frequencies for **5** occur at 1063 and 1024 cm^{-1} indicating ionic perchlorate. Metal-chloride bond frequencies for **1** appear in the near-IR region, not observable here due to instrumental limitations. Tables 1 and 2 show the stretching frequencies of the nitrate and carboxylate complexes, respectively. FTIR spectra of all complexes are shown in Figures 8-16.

Table 1. FTIR stretching frequencies of **2**, **3** and **4**.

Compound	$\nu_{nitrate}$ **(cm^{-1})**
$[Co(4\text{-pytpbn})(NO_3)_2]\cdot 6H_2O$	1384
$[Cd(4\text{-pytpbn})(NO_3)_2]\cdot H_2O$	1384, 1298
$[Cu(4\text{-pytpbn})(NO_3)_2]\cdot 5H_2O$	1428,1384, 1226

Table 2. FTIR stretching frequencies of **6**, **7**, **8** and **9**.

Compound	$\nu_{carboxylate}$ **(cm^{-1})**
$[Zn_2(adc)_2(4\text{-pytpbn})]\cdot 6H_2O$	1618 ($\nu_{asymm.}$, COO^-), 1332 ($\nu_{symm.}$, COO^-)
$[Cd_2(adc)_2(4\text{-pytpbn})]\cdot 4H_2O$	1616 ($\nu_{asymm.}$, COO^-), 1364 ($\nu_{symm.}$, COO^-)
$[Ni_2(fum)_2(4\text{-pytpbn})]\cdot 6H_2O$	1558 ($\nu_{asymm.}$, COO^-), 1385 ($\nu_{symm.}$, COO^-)
$[Ni_2(succ)_2(4\text{-pytpbn})]\cdot 4H_2O\cdot 3CH_3OH$	1561 ($\nu_{asymm.}$, COO^-), 1425 ($\nu_{symm.}$, COO^-)

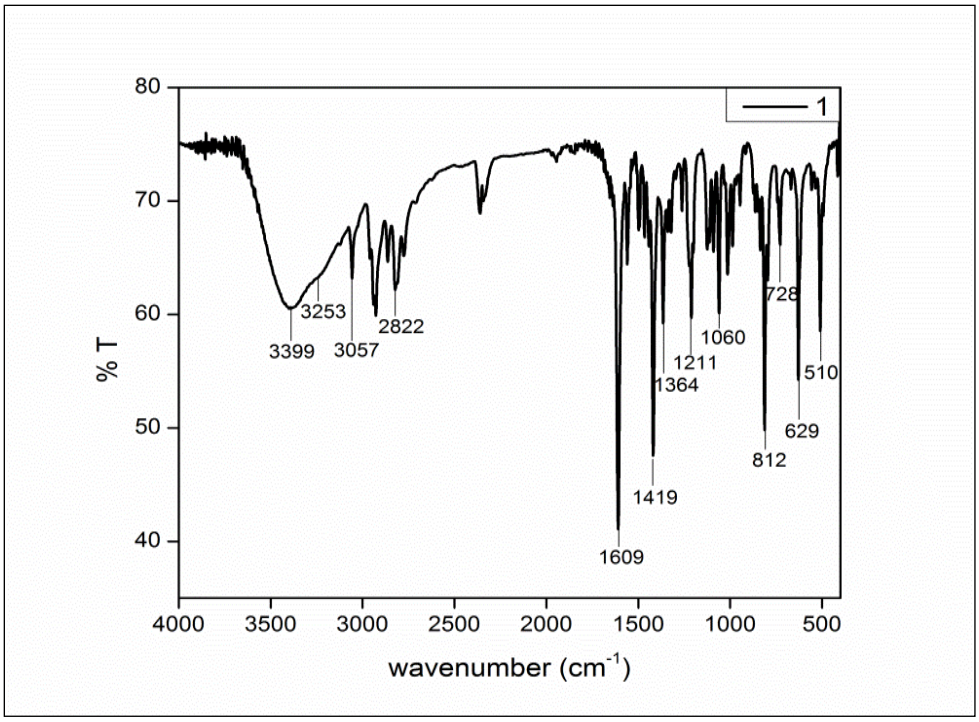

Figure 8. FTIR of $[Co(4\text{-pytpbn})Cl_2]\cdot H_2O$ (**1**).

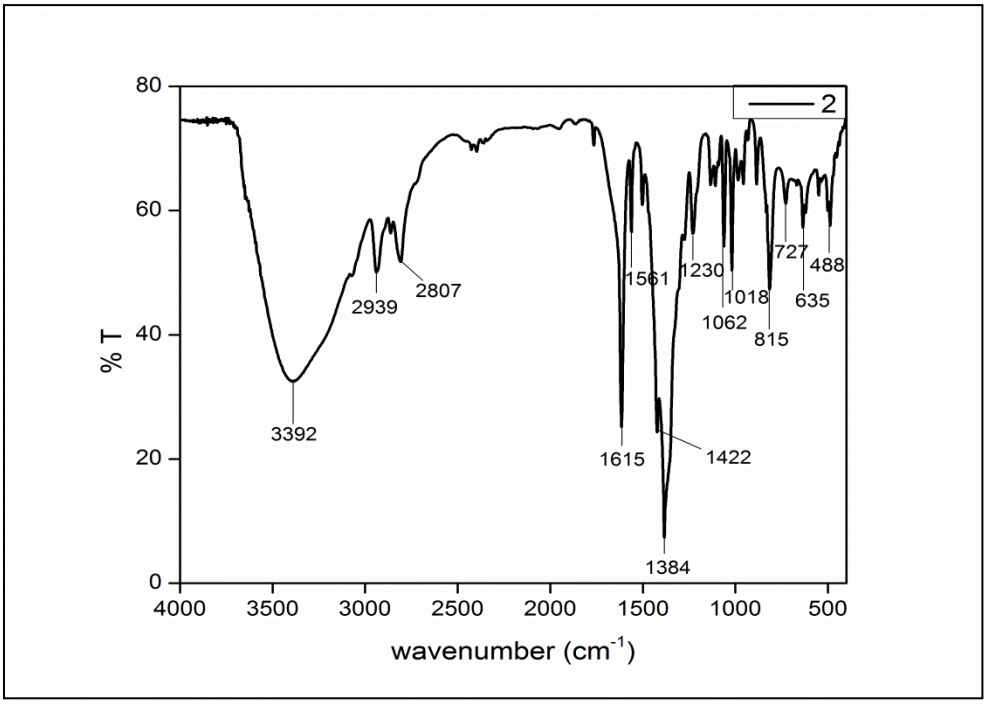

Figure 9. FTIR of $[Co(4\text{-pytpbn})(NO_3)_2]\cdot 6H_2O$ (**2**).

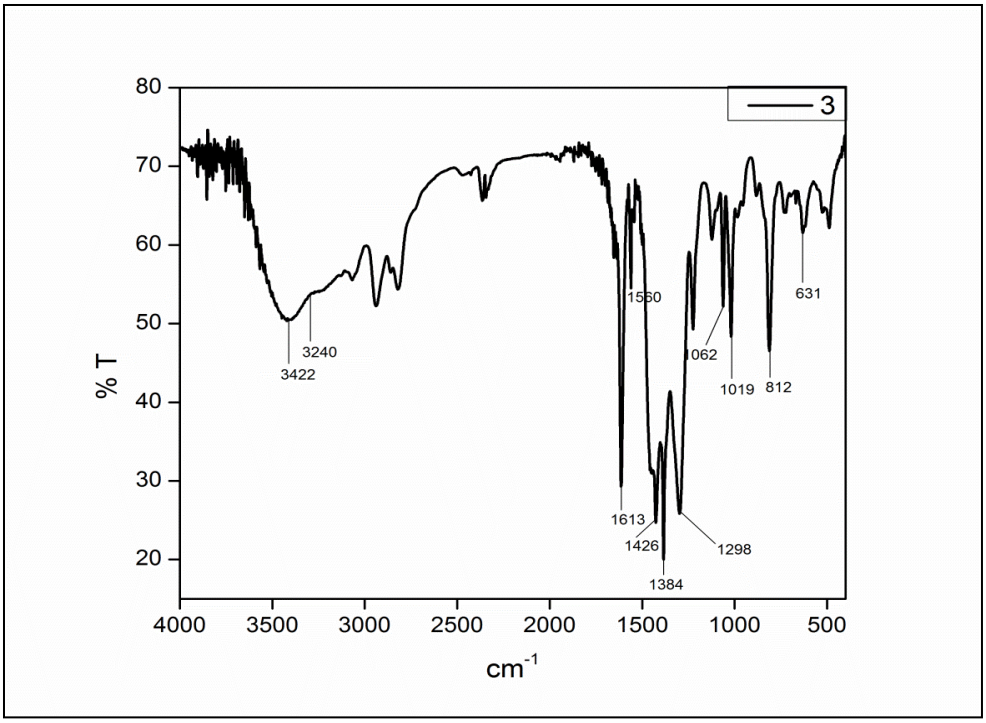

Figure 10. FTIR of $[Cd(4\text{-pytpbn})(NO_3)_2]\cdot H_2O$ (**3**).

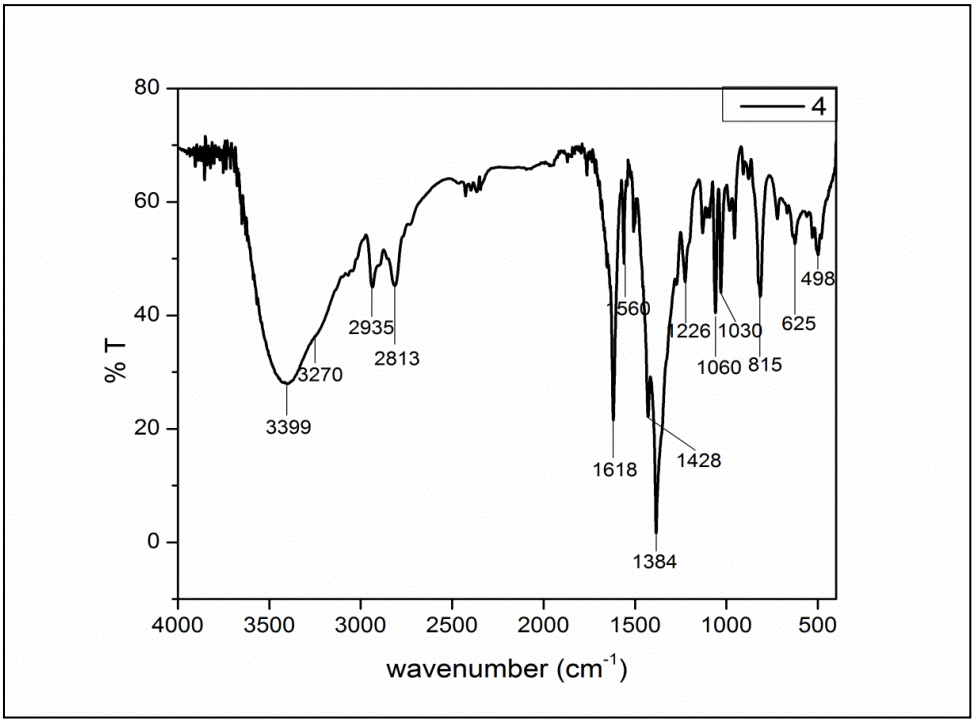

Figure 11. FTIR of $[Cu(4\text{-pytpbn})(NO_3)_2]\cdot 5H_2O$ (**4**).

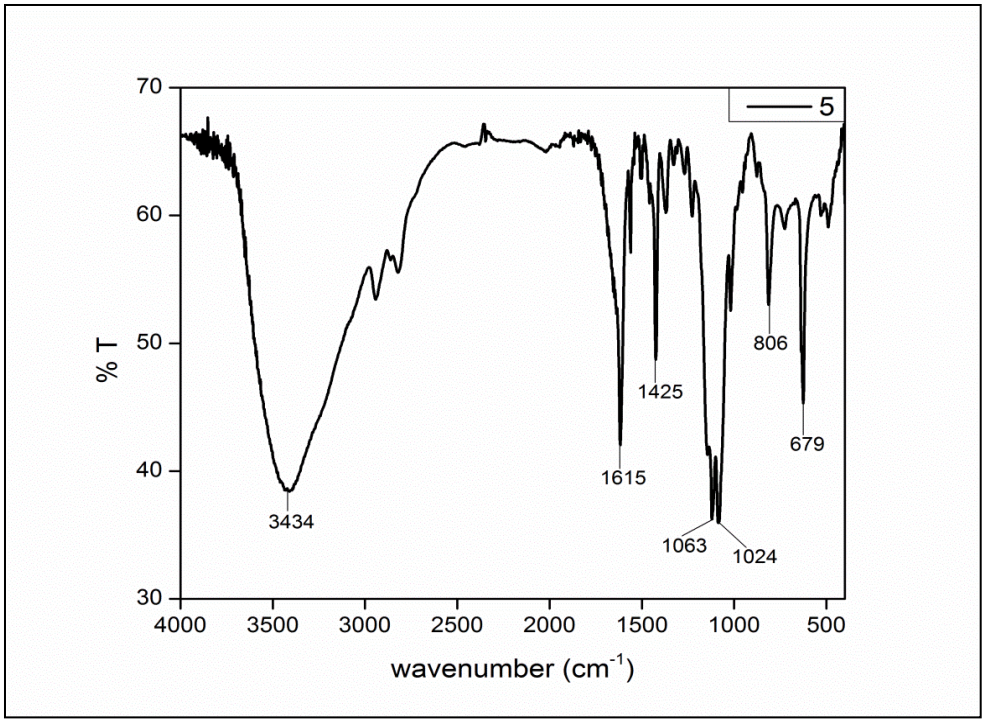

Figure 12. FTIR of $[Co(4\text{-pytpbn})(ClO_4)_2]\cdot 8H_2O$ (**5**).

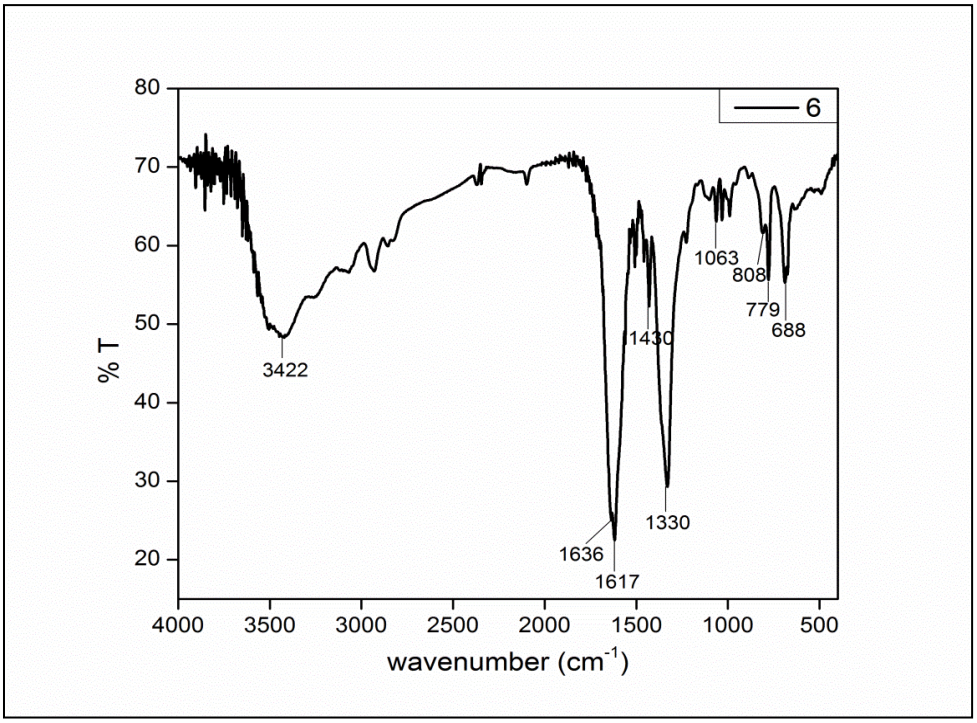

Figure 13. FTIR of $[Zn_2(adc)_2(4\text{-pytpbn})]\cdot 6H_2O$ (**6**).

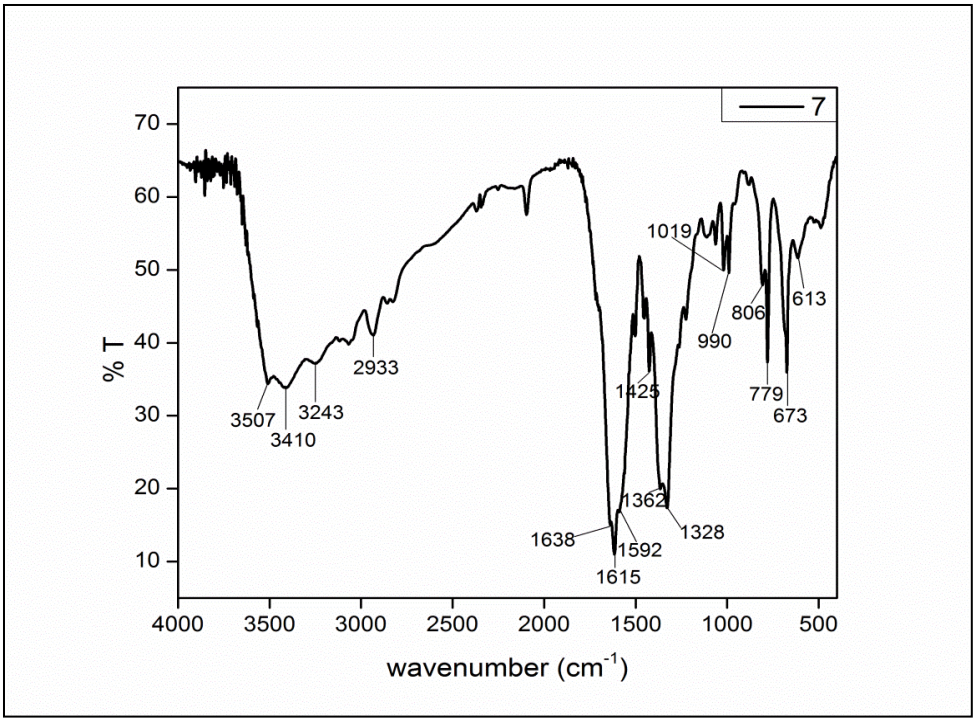

Figure 14. FTIR of $[Cd_2(adc)_2(4\text{-pytpbn})]\cdot 4H_2O$ (**7**).

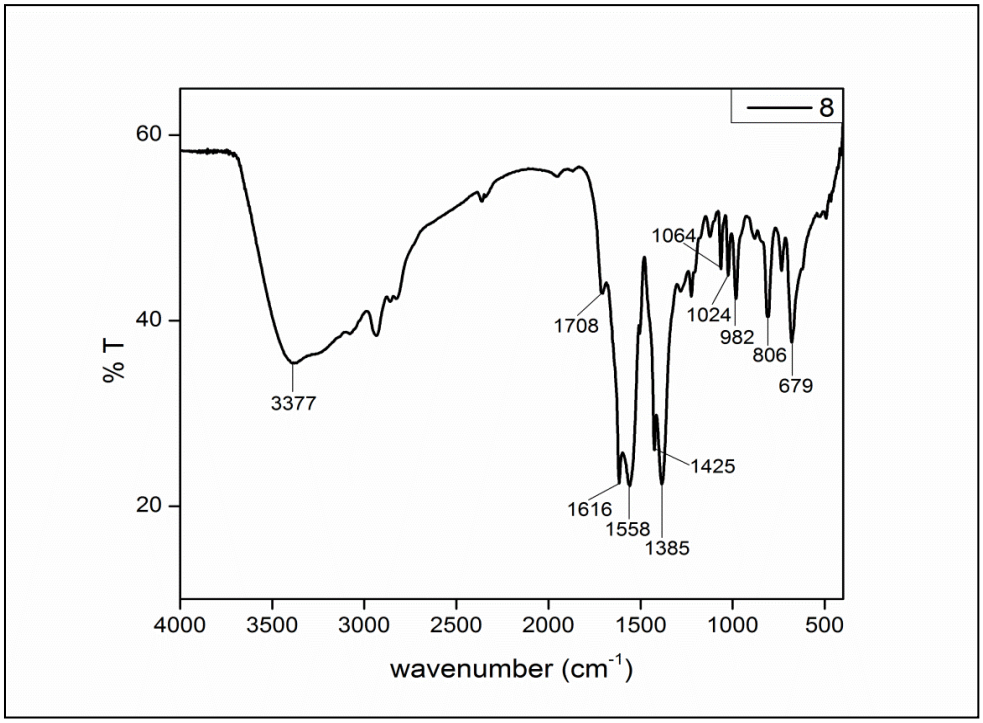

Figure 15. FTIR of $[Ni_2(fum)_2(4\text{-pytpbn})]\cdot 6H_2O$ (**8**).

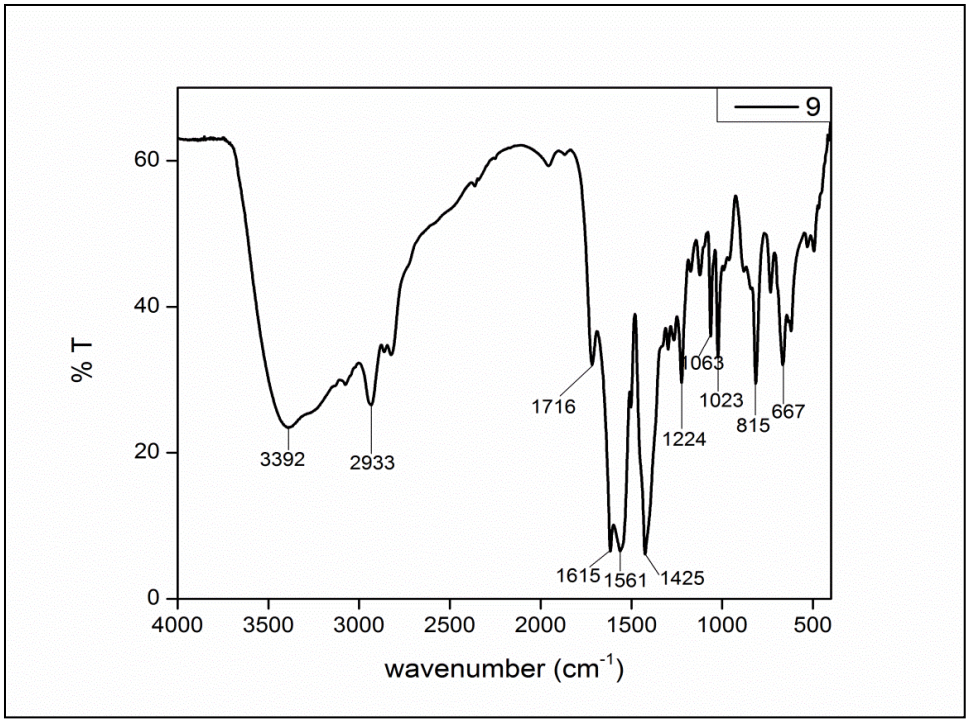

Figure 16. FTIR of $[Ni_2(succ)_2(4\text{-pytpbn})]\cdot 4H_2O\cdot 3CH_3OH$ (**9**).

Single Crystal X-ray Analysis

Single crystals of the ligands were obtained by slow evaporation of their ethyl acetate solutions and those of metal complexes **1** and **2** were grown by direct layering of the reactants. The ligand 4-pytpbn shows the formation of supramolecular assembly through intermolecular π-π interaction. The 2,4-py derivative, however, does not show any π-π interactions. The 4-pyridyl rings in 4-pytpbn are oriented trans to each other on the two aliphatic nitrogens, respectively. Similar is the case with the 2-pyridyl and 4-pyridyl rings in 2,4-pypbn. The crystal structures of 4-pytpbn and 2,4-pytpbn are shown in Figures 17 and 19, respectively. The supramolecular assembly in 4-pytpbn is shown in Figure 18. Selected bond lengths and angles for both are summarized in Table 4.

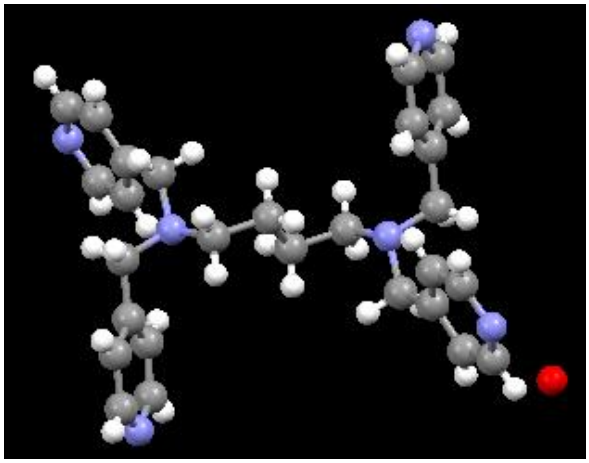

Figure 17. Crystal structure of 4-pytpbn.

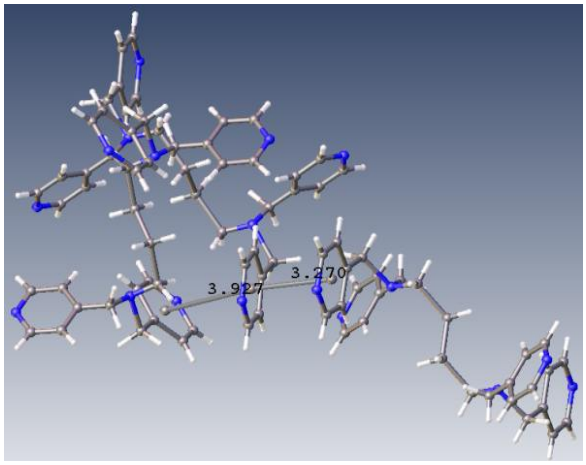

Figure 18. Supramolecular assembly in 4-pytpbn.

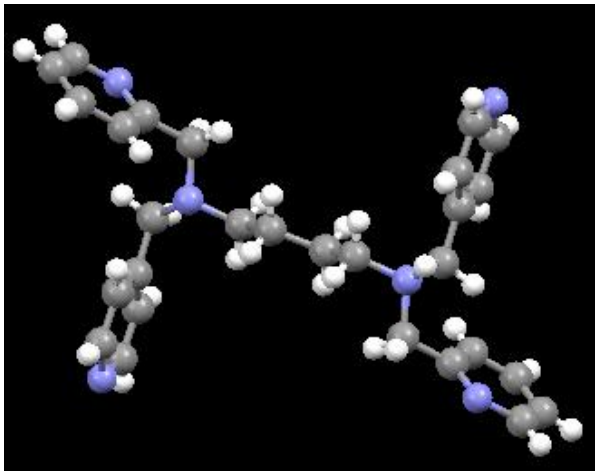

Figure 19. Crystal structure of 2,4-pytpbn.

Table 3. Crystal structure data and refinement parameters for 4-pytpbn and 2,4-pytpbn.

Compound	**4-pytpbn**	**2,4-pytpbn**
Chemical Formula	$C_{28}H_{34}N_6O$	$C_{28}H_{32}N_6$
Formula Weight	470.61	452.6
Temperature (K)	296(2)	296(2)
Wavelength (Å)	0.71073	0.71073
Crystal System	Orthorhombic	Triclinic
Space Group	P*nna*	P -1
a (Å)	10.786(3)	5.956(10)
b (Å)	17.920(5)	9.540(16)
c (Å)	14.260(4)	12.15(2)
a (°)	90	108.59(3)
β (°)	90	93.55(2)
g (°)	90	94.50(2)
Z	4	1
V ($Å^3$)	2756.2(13)	649.6(19)
Density (mg/cm^3)	1.134	1.157
μ(mm^{-1})	0.72	0.071
F(000)	1008	242
Theta Range for Data Coll.	1.83 to 25.01˚	1.78 to 22.23˚
Reflections Collected	28772	4743
Independent Reflections	2433	1593
Reflections with I >2σ(I))	1184	904
R_{int}	0.0456	0.0283
No. of Parameters refined	163	155
GOF on F^2	1.085	0.922
Final R_1[a]/wR_2[b] (I >2σ(I))	0.0913/0.2744	0.0545/0.1554
R_1[a]/wR_2[b] (all data)	0.1553/0.3318	0.0944/0.1857
Largest diff. peak and hole($eÅ^{-3}$)	0.724 and -0.182	0.141 and -0.188

[a]$R_1 = \Sigma||Fo| - |Fc||/\Sigma|Fo|$. [b]$wR_2 = [\Sigma w(Fo^2 - Fc^2)^2/\Sigma w(Fo^2)^2]^{1/2}$, where $w = 1/[\sigma^2(Fo^2) + (aP)^2 + bP]$, $P = (Fo^2 + 2Fc^2)/3$.

Table 4. Selected bond distances (Å) and bond angles (º) for 4-pytpbn and 2,4-pytpbn.

Bond Distances

	4-pytpbn	**2,4-pytpbn**
N_{ali}-$CH_{2\ (4\text{-}py)}$	1.449(5), 1.473(5)	1.478(4)
N_{ali}-$CH_{2\ (2\text{-}py)}$	-	1.472(4)
N_{ali}-C_{ali}	1.476(4)	1.478(4)

Bond Angles

	4-pytpbn		**2,4-pytpbn**
$CH_{2\ (4\text{-}py)}$-N_{ali}-$CH_{2\ (4\text{-}py)}$	110.2(3)	$CH_{2\ (4\text{-}py)}$-N_{ali}-$CH_{2\ (2\text{-}py)}$	110.8(3)
$CH_{2\ (4\text{-}py)}$-N_{ali}-C_{ali}	109.8(3), 111.4 (3)	$CH_{2\ (4\text{-}py)}$-N_{ali}-C_{ali}	111.0(3)
		$CH_{2\ (2\text{-}py)}$-N_{ali}-C_{ali}	111.5(2)

Single crystals of **1** and **2** were found to be marginal and thus finalization of their structures requires a lot more effort. Preliminary results that are obtained for **1** and **2** are shown below:

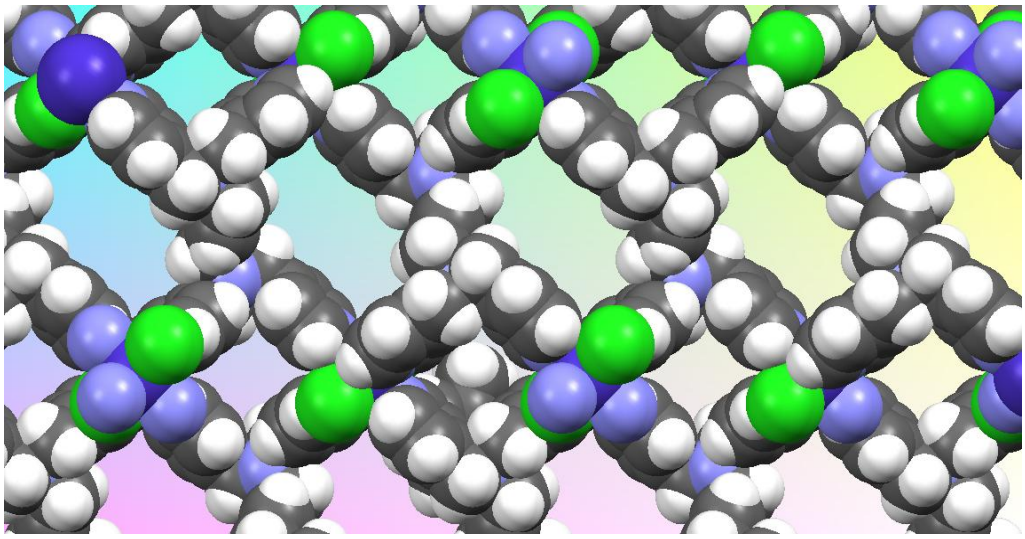

Figure 20. A perspective view of pores in **1.**

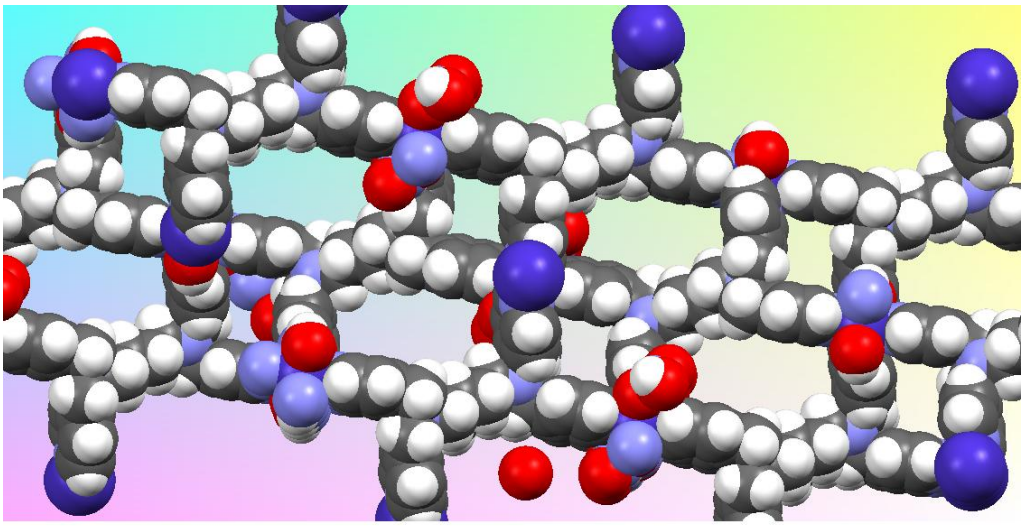

Figure 21. A perspective view of pores in **2.**

Powder X-ray Diffraction (PXRD) Studies

Powder X-ray diffraction was used to analyze the ligand and complexes to check their crystalline nature. The ligand 4-pytpbn shows good crystalline behavior (Figure 22). Only complexes **1**, **2**, **4**, **5** and **7** show some crystallinity, all other complexes are amorphous. Complexes **1**, **2** and **5** are isostructural, as evident from their PXRD patterns (Figure 23). Figures 24 and 25 show the PXRD patterns of complexes **4** and **7**, respectively.

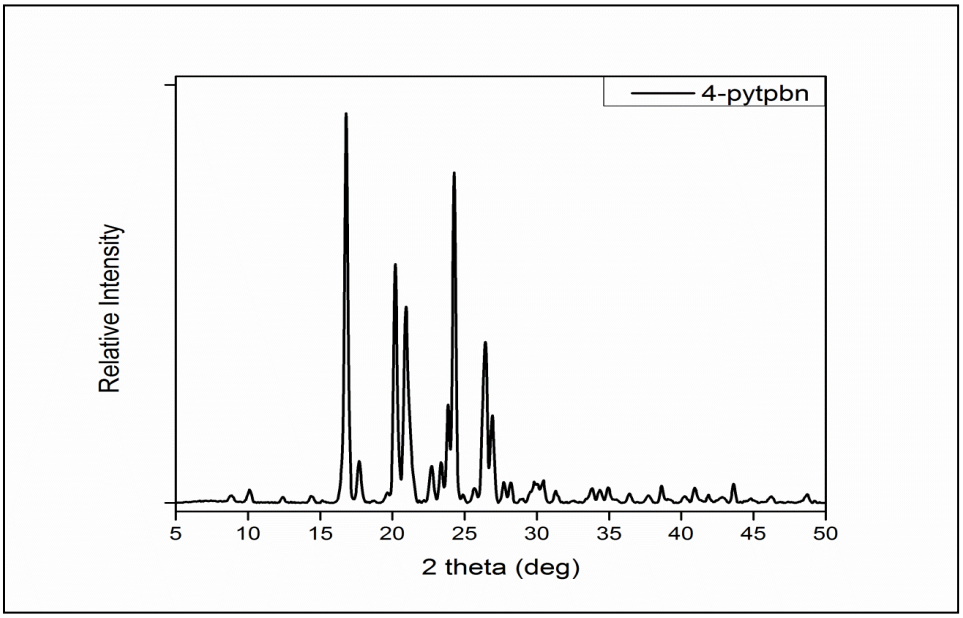

Figure 22. Powder diffraction pattern of 4-pytpbn.

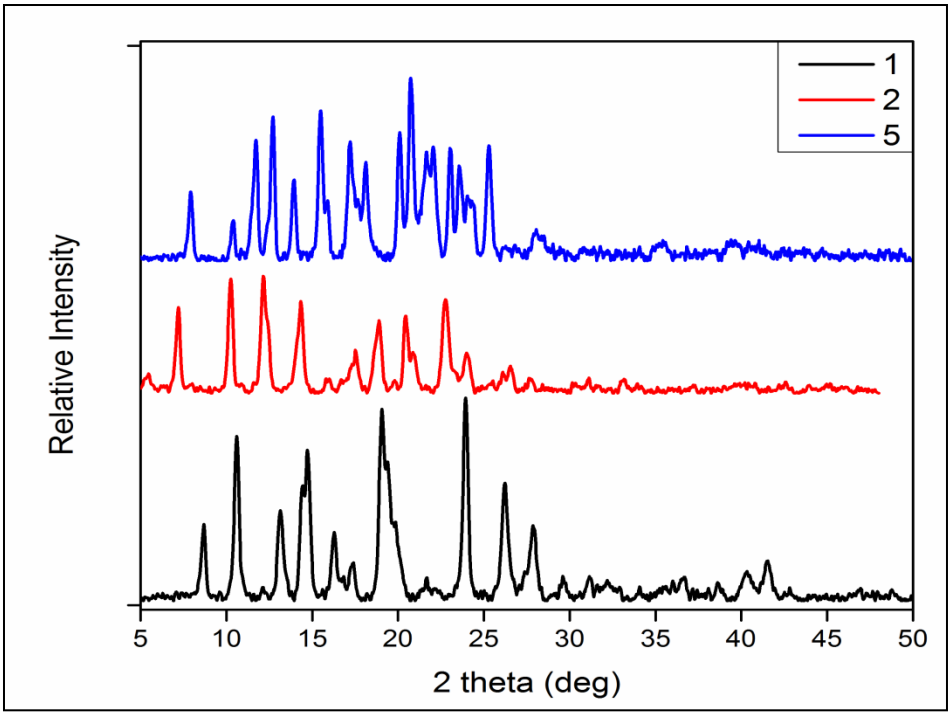

Figure 23. Comparison of powder diffraction patterns of **1**, **2** and **5**.

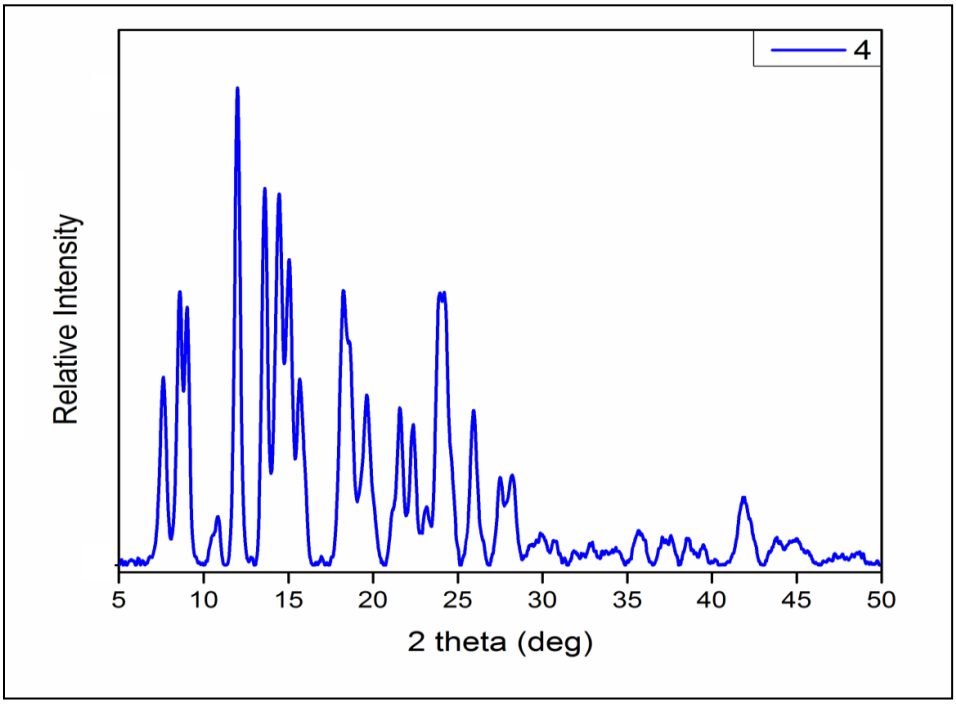

Figure 24. Powder diffraction pattern of **4**.

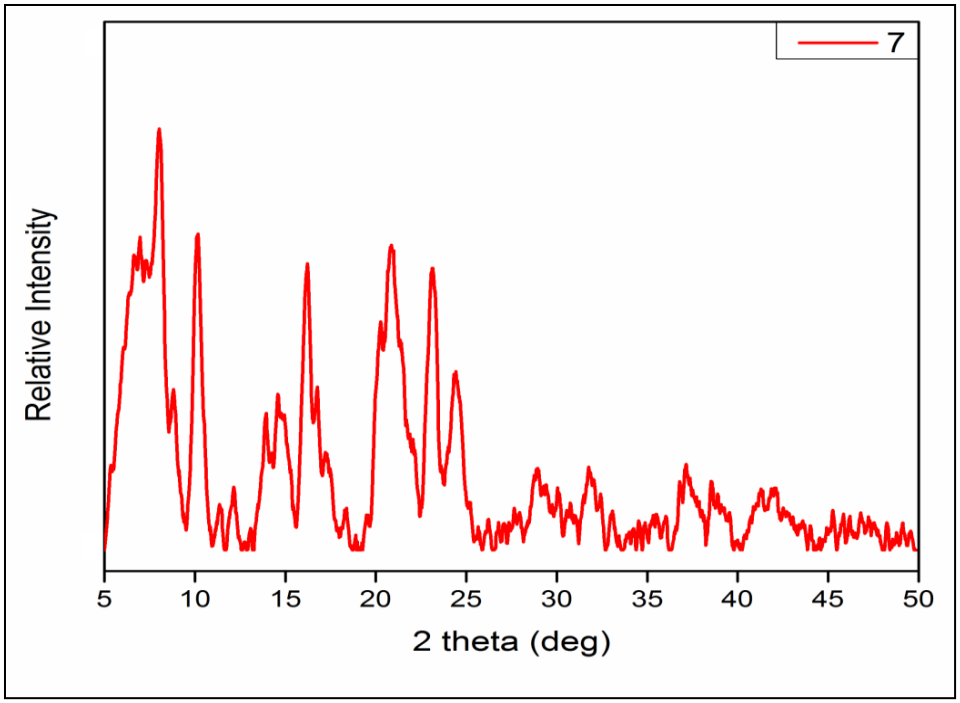

Figure 25. Powder diffraction pattern of **7**.

Thermal Properties

In order to study their thermal stabilities, all compounds were examined by thermogravimetric analysis (TGA) between 25-500 ºC. The ligand is stable up to 280 ˚C as shown in Figure 26. Complex **1** is stable up to 200 ˚C after initial loss of one water molecule at 100 ˚C (Figure 27). Complexes **2**, **3** and **4** are quite stable up to 200 ˚C showing loss of solvent molecules initially around 100 ˚C followed by loss of nitrate ions and the ligand in the subsequent steps (Figure 28). Complex **3** is the most stable among these, as decomposition after initial loss of solvent starts only at 250 ˚C. Complexes **6**, **7**, **8** and **9** show continuous weight loss and thus exact loss of the components is difficult to establish (Figure 29). Complex **5** is a perchlorate salt, and thus was not analysed.

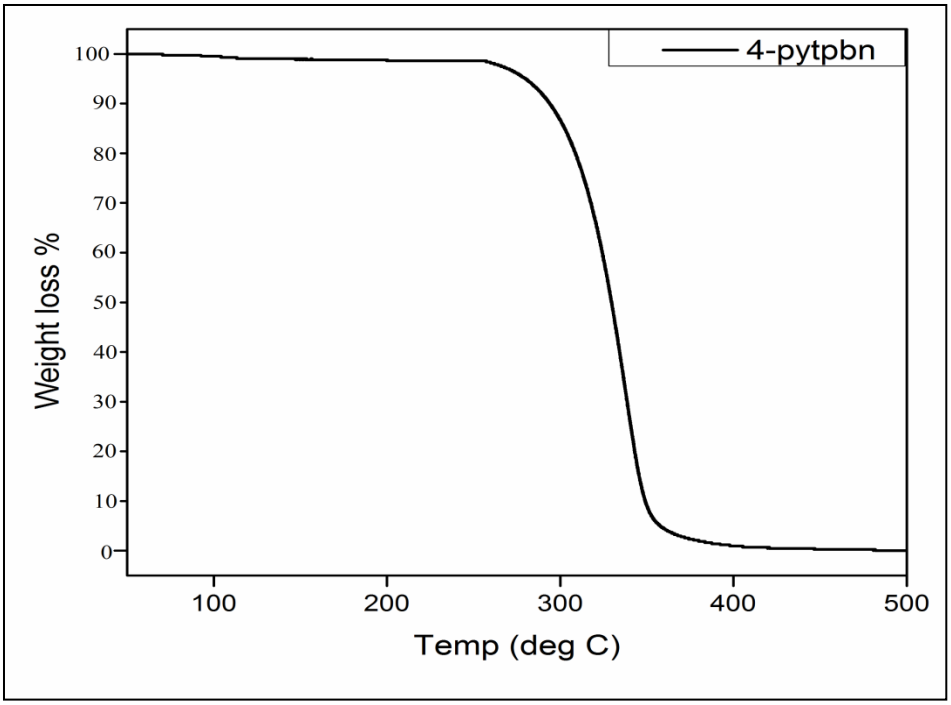

. **Figure 26.** TGA scan of 4-pytpbn.

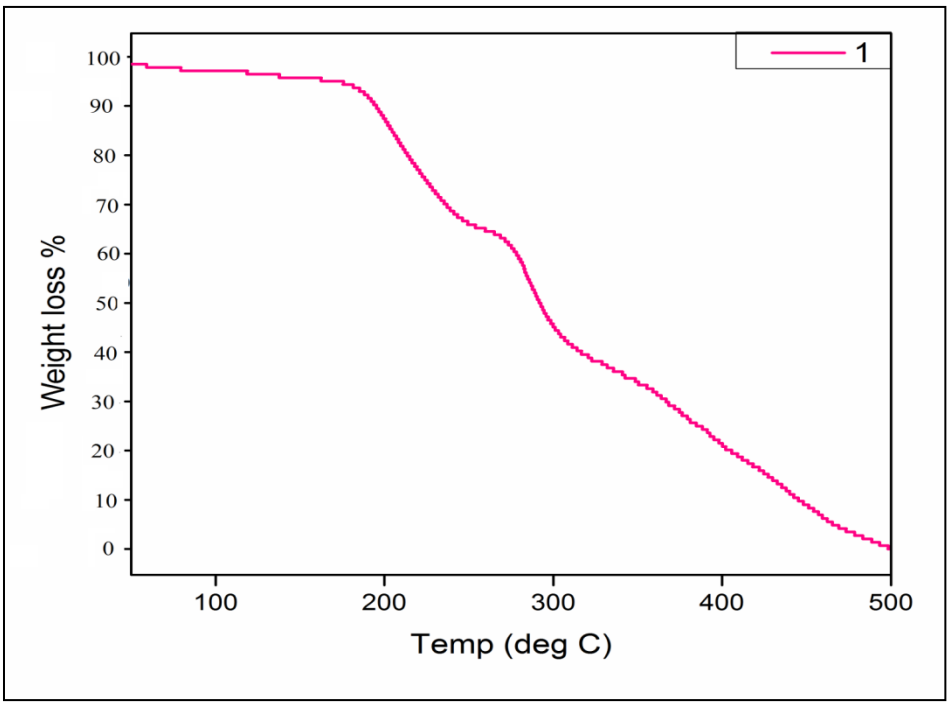

Figure 27. TGA scan of **1.**

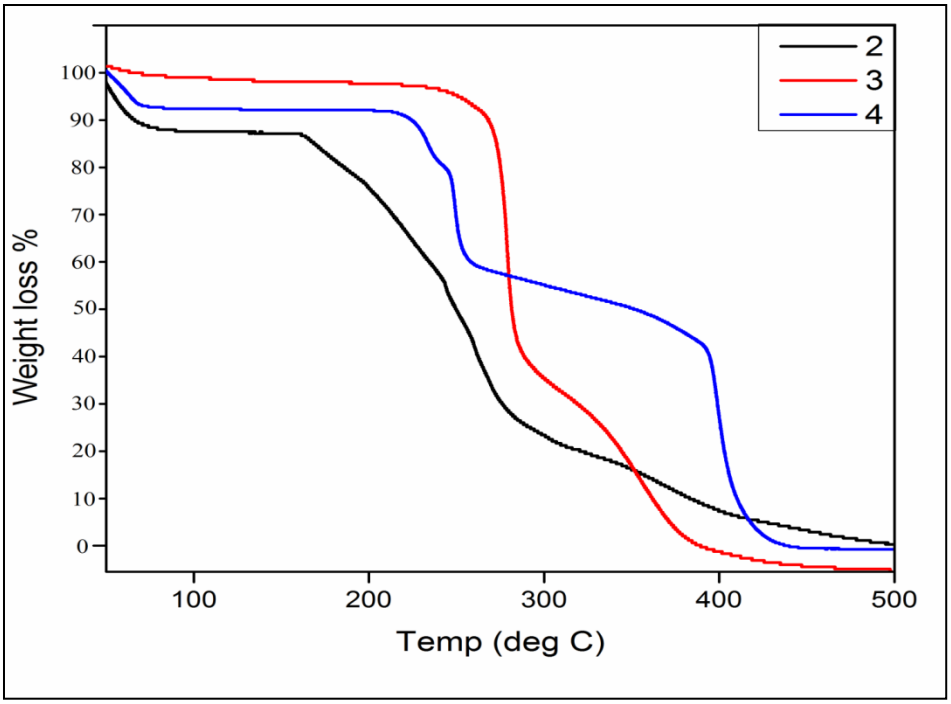

Figure 28. TGA scans of **2**, **3** and **4**.

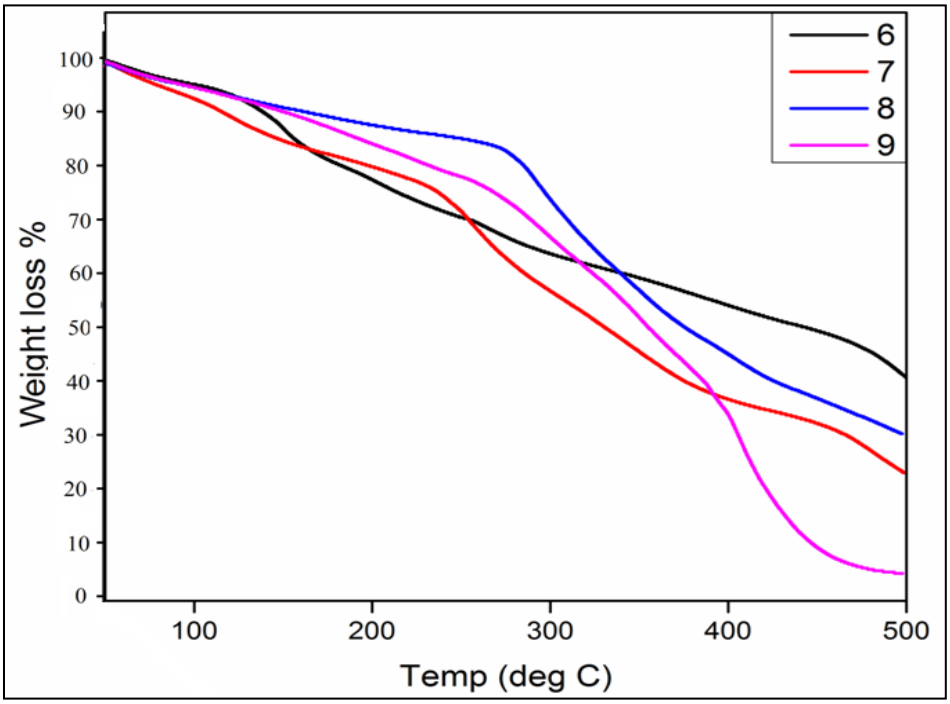

Figure 29. TGA scans of **6**, **7**, **8** and **9.**

Chapter IV

Conclusions and Future Directions

In this work, two hexadentate ancillary ligands, 4-pytpbn and 2,4-pytpbn, were synthesized and structurally characterized. Their spectroscopic properties corroborates well with the solid state structures determined by single crystal X-ray diffractometry. Nine metal complexes of 4-pytpbn both with and without the linkers were synthesized and characterized by a number of analytical techniques. Preliminary single crystal X-ray structures of complexes **1** and **2** show the formation of porous 3-D networks. Thermal properties of the 4-pytpbn ligand and the metal complexes (wherever possible) were compared.

For 4-pytpbn, the addition of sodium triacetoxyborohydride in two portions at an interval of 24 h has shown to give better yields. Thus increasing the number of portions can be tried. For the 2,4-derivative, the yield obtained in the first step of the synthesis is good, the second step needs to be optimized, possibly with a change in the time interval of addition of sodium hydroxide.

Single crystals of the complexes **1** and **2** were obtained by direct layering of the two reactants, but results with these are marginal and further structural refinement needs to be done. Also, since these are soluble in DMSO, water/methanol and water/acetonirile mixtures, recrystallization by slow evaporation of solvent can be tried. The nitrate and chloride salts of nickel(II), manganese(II) and cadmium(II) can also be tried for direct layering. Metal complexes of 2,4-pytpbn can be done with cobalt(II) nitrate, cobalt(II) chloride and cobalt(II) perchlorate for structural comparison. Other metals such as cadmium(II), nickel(II), manganese(II), etc., can also be used.

Further crystal growth of other complexes for structural elucidation is required and once the structures of these complexes are fully established, extensive studies can be done for their applications in gas adsorption, storage and separation. Also, catalyst systems based on triazine derivatives[49] and other multidentate polypyridyl ligands for stability have been reported for photocatalytic production of dihydrogen.[50] Metal complexes reported in this work can be tried for such applications and also for C-C bond formation, C-H activation, etc.[51] Other applications, such as selective metal ion complexation and sensing, can also be examined.[52]

References

1. Rosi, N. L.; Eddaoudi, M.; Kim, J.; O'Keeffe, M.; Yaghi, O. M. *CrystEngComm* **2002**, *4*, 401.
2. (a) Kauffman, G. B. *Coord. Chem. Rev.* **1972**, *9*, 339; (b) James, K. B. *Acc. Chem. Res.* **2005**, *38*, 671.
3. Shibata, Y. *J. Coll. Sci. Imp. Univ. Tokyo* **1916**, *37*, 1.
4. (a) Rayner, J. H.; Powell, H. M. *J. Chem. Soc.* **1952**, 319; (b) Hasegawa, T.; Nishikiori, S.; Iwamoto, T. *Chem. Lett.* **1985**, 1659.
5. Hoskins, B. F.; Robson, R. *J. Am. Chem. Soc.* **1989**, *111*, 5962.
6. Abrahams, B. F.; Hoskins, B. F.; Michail, D. M.; Robson, R. *Nature* **1994**, *369*, 727.
7. Kitagawa, S.; Kawata, S.; Kondo, M.; Nozaka, Y.; Munakata, M. *Bull. Chem. Soc. Jpn.* **1993**, *66*, 3387.
8. Fujita, M.; Kwon, Y. J.; Washizu, S.; Ogura, K. *J. Am. Chem. Soc.* **1994**, *116*, 1151.
9. Subramanian, S.; Zaworotko, M. J. *Angew. Chem. Intl. Ed.* **1995**, *34*, 2127.
10. Yaghi, O. M.; Li, H. *J. Am. Chem. Soc.* **1995**, *117*, 10401.
11. Hirsch, K. A.; Wilson, S. R.; Moore, J. S. *J. Am. Chem. Soc*. **1997**, *119*, 10401.
12. Yaghi, O. M.; Li, G.; Li, H. *Nature*, **1995**, *378*, 703.
13. Kondo, M.; Okubo, T.; Asami, A.; Noro, S. I.; Yoshitomi, T.; Kitagwa, S.; Ishii, T.; Matsuzaka, H.; Seki, K. *Angew. Chem. Intl. Ed.* **1999**, *38*, 140.
14. Kuppler, R. J.; Timmons, D. J.; Fang, Q. R.; Li, J. R.; Makal, T. A.; Young, M. D.; Yuan, D.; Zhao, D.; Zhuang, W.; Zhou, H .C. *Coord. Chem. Rev.* **2009**, *253*, 3042.
15. Batten, S. R.; Champness, N. R.; Chen, X. M.; Garcia-Martinez, J.; Kitagawa, S.; Ohrstrom, L.; O′ Keeffe, M.; Suh, M. P.; Reedijk, J. *Pure Appl. Chem.* **2013**, *85*, 1715.
16. The IUPAC Project "Coordination Polymers and Metal Organic Frameworks: Terminology and Nomenclature Guidelines", www.iupac.org/web/ins/2009-012-2-200.
17. (a) Khullar, S.; Mandal, S. K. *Cryst. Growth Des.*, **2012**, *12*, 5329; (b) Khullar, S.; Mandal, S. K. *Cryst. Growth Des.* **2013**, *13*, 3116; (c) Khullar, S.; Gupta, V.; Mandal, S. K. *CrystEnggComm*. **2014**, doi: 10.1039/x0xx00000x.
18. (a) Marisa Faraggi et al. *J. Phys. Chem. C* **2012**, *116*, 24558; (b) Christopher Kley et al. *J. Am. Chem. Soc.* **2012**, *134*, 6072.

19. Kitagawa, S.; Kitaura, R.; Noro, S. *Angew. Chem. Int. Ed.* **2004**, *43*, 2334.
20. Wriedt, M.; Zhou, H. C. *Dalton Trans.* **2012**, *41*, 4207.
21. (a) Pan, L.; Adams, K. M.; Hernandez, H. E.; Wang, X.; Zheng, C.; Hattori, Y.; Kaneko, K. *J. Am. Chem. Soc.* **2003**, *125*, 3062; (b) Reineke, T. M.; Eddaoudi, M.; Fehr, M.; Kelley, D.; Yaghi, O. M. *J. Am. Chem. Soc.* **1999**, *121*, 1651.
22. (a) Hagrman, P. J.; Hagrman, D.; Zubieta, J. *Angew. Chem. Int. Ed.* **1999**, *38*, 2639; (b) Moulton, B.; Zaworotko, M. J. *Chem. Rev.* **2001**, *101*, 1629; (c) Zaworotko, M. J. *Chem. Commun.* **2001**, 1.
23. (a) Song,P.; Liu, B.; Li, Y. Q.; Yang, J. Z.; Wang, Z. M.; Li, X. G. *CrystEngComm.* **2012**, *14*, 2296; (b) Pachfule, P.; Panda,T.; Dey, C.; Banerjee, R. *CrystEngComm*. **2010**, *12*, 2381.
24. Eddaoudi, M.; Moler, D. B.; Li, H. L.; Chen, B. L.; Reineke, T. M.; O'Keeffe, M.; Yaghi, O. M. *Acc. Chem. Res.*, **2001**, *34*, 319; (b) Gutschke, S.O.H.; Price, D. J.; Powell, A. K.; Wood, P. T. *Angew. Chem. Int. Ed.* **2001**, *40*, 1920; (c) Prior, T.J.; Rosseinsky, M. J. *Chem. Commun.* **2001**, 495; (d) Yaghi, O.M.; Li, H. L.; Groy, T. L. *J. Am. Chem. Soc.* **1996**, *118*, 9096; (e) Kumagai, H.; Kepert, C. J.; Kurmoo, M. *Inorg. Chem.* **2002**, *41*, 3410; (f) Kosal, M. E.; Chou, J. H.; Wilson, S. R.; Suslick, K. S. *Nat. Mater.* **2002**, *1*, 118.
25. (a) Zhang, J.; Matsushita, M. M.; Kong, X. X.; Abe, J.; Iyoda, T. *J. Am. Chem. Soc.* **2001**, *123*, 12105; (b) Davidson, G.J.E.; Loeb, S. J. *Angew. Chem. Int. Ed.* **2003**, *42*, 74; (c) Lee, E. S.; Heo, J.S.; Kim, K. *Angew. Chem.Int. Ed.* **2000,** *39*, 2699.
26. Lee, Y. R.; Kim, J.; Ahn, W. S. *Korean J. Chem. Eng.* **2013**, *30*, 1667.
27. (a) Huang, L.; Wang, H.; Chen, J.; Wang, Z.; Sun, J.; Zhao, D.;Yan, Y. *Microporous Mesoporous Mater.* **2003**, *58*, 105; (b) Tranchemontagne, D.; Hunt, J.; Yaghi, O. M. *Tetrahedron* **2008**, *64*, 8553; (c) Cravillon, J.; Munzer, S.; Lohmeier, S. J.; Feldhoff, A.; Huber,K.; Wiebcke, M. *Chem. Mater.* **2009**, *21*, 1410.
28. Furukawa, H.; Cordova, K. E.; O′ Keeffe, M.; Yaghi, O. M. *Science* **2013**, *341*, 1230444.
29. Rosi, N. L.; Eckert, J.; Eddaoudi, M.; Vodak, D. T.; Kim, J.; O'Keeffe, M.; Yaghi, O. M. *Science* **2003**, *300*, 1127.
30. Zhao, D.; Yuan, D. Q.; Zhou, H. C. *Energy Environ. Sci.* **2008**, *1*, 222.
31. (a) Wong-Foy, A. G.; Matzger, A. J.; Yaghi, O. M. *J. Am. Chem. Soc.* **2006**, *128*, 3494;

(b) Furukawa, H.; Miller, M. A.; Yaghi, O. M. *J. Mater. Chem.* **2007**, *17*, 3197.

32. Millward, A. R.; Yaghi, O. M. *J. Am. Chem. Soc.* **2005**, *127*, 17998; (b) Llewellyn, P. L.; Bourrelly, S.; Serre, C.; Vimont, A.; Daturi, M.; Hamon, L.; De Weireld, G.; Chang, J.S.; Hong, D. Y.; Hwang, Y. K.; Jhung, S. H.; Ferey, G. *Langmuir* **2008**, *24*, 7245.
33. Bae, Y. S.; Farha, O. K.; Hupp, J. T.; Snurr, R. Q. *J. Mater. Chem.* **2009**, *19*, 2131; (b) Demessence, A.; D'Alessandro, D. M.; Foo, M. L.; Long, J. R. *J. Am. Chem. Soc.* **2009**, *131*, 8784.
34. Guo, H.; Zhu, G.; Hewitt, I. J.; Qiu, S. *J. Am. Chem. Soc.* **2009**, *131*, 1646.
35. Gándara, F.; Gornez-Lor, B.; Gutiérrez-Puebla, Iglesias, E. M.; Monge, M. A.; Proserpio, D. M.; Snejko, N. *Chem. Mater.* **2008**, *20*, 72.
36. Horcajada, P.; Serre, C.; Maurin, G.; Ramsahye, N. A.; Balas, F.; Vallet-Regi, M.; Sebban, M.; Taulelle, F.; Férey, G. *J. Am. Chem. Soc.* **2008**, *130*, 6774.
37. Shi, Z.; Lin, N. *J. Am. Chem. Soc.* **2010**, *132*, 10756.
38. Dmitriev, A.; Spillmann, H.; Lin, N.; Barth, J. V.; Kern, K. *Angew. Chem. Int. Ed.* **2003**, *42*, 2670.
39. Toftlund, H.; Murray, K. S.; Zwack, P. R.; Taylor, L. F.; Anderson, O. P. *J. Chem. Soc., Chem. Comm.* **1986**, 191.
40. Jensen, K. B.; McKenzie, C. J.; Simonsen, O.; Toftlund, H.; Hazell, A. *Inorg. Chim. Acta* **1997**, *257*, 163.
41. Neves, A.; Vencato, I.; Horner, M.; Fenner, H.; Strahle, J. *J. Braz. Chem. Soc.* **1995**, *6(3)*, 261.
42. Mambanda, A.; Jaganyi, D.; Hochreuthe, S.; van Eldik, R. *Dalton Trans.* **2010**, *39*, 3595.
43. Hofmann, A.; van Eldik, R. *Dalton Trans.* **2003**, 2979.
44. Fujihara, T.; Saito, M.; Nagasawa, A. *Acta Cryst.* **2004**, *E60*, o262.
45. APEX2, SADABS and SAINT; Bruker AXS Inc.: Madison, WI, USA, 2008.
46. Sheldrick, G. M. *Acta Crystallogr.***2008**, *A64*, 112.
47. Macrae, C. F.; Bruno, I. J.; Chisholm, J. A.; Edginton, P. R.; McCabe, P.; Pidocck, E.; Rodriguez-Monge, L.; Taylor, T.; Van de Streek, J.; Wood, P. A. *J. Appl. Crystallogr.* **2008**, *41*, 266.
48. Spek, A. L. PLATON, Version 1.62; University of Utrecht: 1999.

49. Gamez, P.; de Hoog, P.; Lutz, M.; Spek, A. L.; Reedijk, J. *Inorg. Chim. Acta* **2003**, *351*, 319.
50. Guttentag, M.; Rodenberg, A.; Bachmann, C.; Senn, A.; Hamm, P.; Alberto, R. *Dalton Trans.* **2013**, *42*, 334.
51. Lee, J. Y.; Farha, O.K.; Roberts, J.; Scheidt, K. A.; Nguyen, S. T.; Hupp, J. T. *Chem. Soc. Rev.* **2009**, *38*, 1450.
52. Hancock, R. D. *Chem. Soc. Rev.* **2013**, *42*, 1500.